Genetics: Early Online, published on April 16, 2020 as 10.1534/genetics.120.303190

# The yeast Hsp70 co-chaperone Ydj1 regulates functional distinction of Ssa Hsp70s in the Hsp90 chaperoning pathway

Deepika Gaur[1], Prashant Singh[1], Jyoti Guleria[1], Arpit Gupta[2], Satinderdeep Kaur[1], Deepak Sharma[1*]

[1]Council of Scientific and Industrial Research-Institute of Microbial Technology, India, [2]Council of Scientific and Industrial Research-Institute of Microbial Technology, India, Currently in Department of Chemistry, M/C 147-75, California Institute of Technology, 1200 E. California Blvd. Pasadena, CA 91125

*__Corresponding author:__ E-mail: deepaks@imtech.res.in, CSIR-Institute of Microbial Technology, Sector 39A, Chandigarh, India.

Phone: 91-172-6665478

**Running Title:** Ydj1 specifies Hsp70 function

**Financial Disclosure:**

The work is supported by Council of Scientific and Industrial Research (CSIR), India and the Rapid Grant for Young Investigators (RGYI) grant (BT/PR6463/GBD/27/420/2012) from Department of Biotechnology, India.

**Conflict of interest:** The authors declare that they have no conflicts of interest.

**Abstract:**

Hsp90 assists in the folding of diverse sets of client proteins including kinases and growth hormone receptors. Hsp70 plays a major role in many Hsp90 functions by interacting and modulating conformation of its substrates before being transferred to Hsp90s for final maturation. Each eukaryote contains multiple members of the Hsp70 family. However, the role of different Hsp70 isoforms in Hsp90 chaperoning actions remains unknown. Using v-Src as an Hsp90 substrate, we examine the role of each of the four yeast cytosolic Ssa Hsp70s in regulating Hsp90 functions. We show that the strain expressing stress-inducible Ssa3 or Ssa4 and the not constitutively expressed Ssa1 or Ssa2 as the sole Ssa Hsp70 isoform reduces v-Src mediated growth defects. The study shows that although different Hsp70 isoforms interact similarly with Hsp90s, v-Src maturation is less efficient in strains expressing Ssa4 as the sole Hsp70. We further show that the functional distinction between Ssa2 and Ssa4 is regulated by its C-terminal domain. Further studies reveal that Ydj1, which is known to assist substrate transfer to Hsp70s, interacts relatively weakly with Ssa4 compared to Ssa2, which could be the basis for poor maturation of the Hsp90 client in cells expressing stress-inducible Ssa4 as the sole Ssa Hsp70. The study thus reveals a novel role of Ydj1 in determining the functional distinction among Hsp70 isoforms with respect to the Hsp90 chaperoning action.

## Introduction:

Heat shock protein 90 (Hsp90) is a highly conserved chaperone across all eukaryotes (CHEN *et al.* 2006). Vertebrates and lower eukaryotes contain multiple highly homologous cytosolic Hsp90 isoforms with only partial functional redundancy (VOSS *et al.* 2000; LI *et al.* 2012). Hsp90 is involved in the folding of various key cellular proteins and is thus essential for cellular survival in eukaryotes. Its client proteins include transcription factors, kinases, telomerase and many viral proteins (RAJAPANDI *et al.* 2000; CITRI *et al.* 2006; KIM *et al.* 2008; SRISUTTHISAMPHAN *et al.* 2018). Several Hsp90 clients also include those involved in carcinogenesis such as p53, and thus the chaperone has been extensively studied for its role in cancer biology (BOYSEN *et al.* 2019; DAHIYA *et al.* 2019). Although Hsp90 influences the maturation of large numbers of cellular proteins, the requirements vary with the substrates. For some substrates such as steroid hormone receptors it is essential for both maturation and maintenance and for others such as kinases, the chaperone is required only during the synthesis and folding into the native state (PICARD *et al.* 1990; XU *et al.* 1999). The diversity of Hsp90 functions is believed to be due to its interaction with various co-chaperones. In spite of extensive research, no sequence or structural motif conserved across different client proteins has been identified and thus how Hsp90 binds and assists in the folding of diverse sets of substrates continues to be under intense investigation (TAIPALE *et al.* 2012).

Hsp90 is a homodimeric protein and each protomer consists of three domains, namely, the N-terminal domain that binds to ATP, the client-binding middle domain that also interacts with other co-chaperones and the MEEVD motif, which contains C-terminal domains required for dimerization and interaction with TPR domains containing co-chaperones (MINAMI *et al.* 1994; PRODROMOU *et al.* 1999; LI *et al.* 2012). The client proteins are known to interact with both the middle and the N-terminal domains of Hsp90 (SATO *et al.* 2000; KARAGÖZ *et al.* 2014). ATP

binding to the N-terminal domain leads to conformational changes in Hsp90 (GRAF *et al.* 2009); through an intermediary stage the chaperone forms a closed state in which the N-terminal domain is dimerized. In this structurally compact state, the ATP is hydrolyzed, which leads to dissociation of the N-terminal domains and the release of ADP followed by a transition of Hsp90 back to the original open conformation. The Hsp90 reaction cycles are regulated by dynamic associations with various co-chaperones which are broadly divided into TPR and non-TPR containing proteins such as Sti1, Cpr7 and Aha1, respectively (CHANG *et al.* 1997; MAYR *et al.* 2000; PANARETOU *et al.* 2002).

Hsp70 is one of the other major cellular chaperones that plays a central role in maturation of Hsp90 client proteins such as transcription factors and protein kinases (KIRSCHKE *et al.* 2014; ROY *et al.* 2015). Hsp70 has its own chaperoning activity and its role in the Hsp90 reaction cycle is for the early folding of Hsp90 client proteins. Any defect in the Hsp70-Hsp90 folding cycle results in ubiquitination and degradation of Hsp90 client proteins (LEU *et al.* 2011; RODINA *et al.* 2013; ROY *et al.* 2015). Hsp70 interacts with Hsp90 through an adaptor molecule (e.g., Sti1 and Hop in yeast and mammals, respectively) that acts as a bridge between the two chaperones. Sti1 bridges the two chaperones via its helical TPR domains that bind to the C-terminal EEVD motif present in Hsp70 and Hsp90 (SCHMID *et al.* 2012; RÖHL *et al.* 2015). In addition to being bridged by the adaptor molecules, the two proteins also exhibit direct interactions (KRAVATS *et al.* 2018). The substrate first interacts with Hsp70 and the partially folded substrate is then transferred to Hsp90 for further maturation. The Hsp90 cycle progresses by its interaction with other co-chaperones such as peptidyl prolyl cis/trans isomerases (DUINA *et al.* 1996; WARTH *et al.* 1997) and SbaI (e.g., homologous to mammalian p23) (SULLIVAN *et al.* 2002; MCLAUGHLIN *et al.* 2006) followed by dissociation of Hsp90 from the Hsp70/Hsp90 complex. The exact role of

Hsp70 in regulating Hsp90 functions is not clearly understood. It is believed that the role of Hsp70 in the Hsp90 chaperone machinery is to stabilize protein substrates in a configuration that can be recognized and bound by Hsp90 (KARAGÖZ *et al.* 2014).

Eukaryotes contain multiple, highly homologous members of cytosolic Hsp70, e.g., the genetically tractable *S. cerevisiae* harbors four cytosolic SSA Hsp70 isoforms (Ssa1-4) (WERNER-WASHBURNE *et al.* 1987). Ssa1 and Ssa2 are constitutively expressed whereas Ssa3 and Ssa4 are expressed only under stress conditions such as high temperature and oxidative stress. (WERNER-WASHBURNE *et al.* 1989). Previous studies have shown that although they are highly homologous, the Ssa isoforms possess both redundant as well as distinct functions (LOTZ *et al.* 2019). It has been shown that cells expressing Ssa2 but not Ssa1 stably propagate one of the yeast prions [URE3] (TIBOR ROBERTS *et al.* 2004). It has been similarly shown that the presence of Ssa3 under heat shock conditions is required to suppress α-synuclein-mediated toxicity (FLOWER *et al.* 2005; GUPTA *et al.* 2018). Although various studies have examined the roles of different Hsp70 isoforms in substrate folding, not much is known about their significance for Hsp90 functions. It is also not clear whether different members of the Hsp70 family function similarly or distinctly in the Hsp90 chaperoning pathway. As Hsp70 is required for the Hsp90 chaperoning function, the differences in the actions of these different Hsp70 isoforms could affect the fates of Hsp90 client proteins.

In the present study, using v-Src as a model Hsp90 client protein, we have investigated the roles of different Ssa Hsp70s in the Hsp90 chaperoning pathway. Our results show that although Ssa1 and Ssa2 stabilize v-Src, its maturation is inhibited in strains expressing Ssa3 or Ssa4 as the sole source of Ssa Hsp70. We show that different Ssa Hsp70 isoforms interact similarly with Hsp90 and that their distinct role in the Hsp90 pathway is due to their different affinities with Hsp40

Ydj1. The present study thus reveals that Ydj1 is required not only to stimulate Hsp70 activity but also in defining their functional specificity in Hsp90 chaperoning activity.

**Results:**

**Hsp90 chaperoning action varies with its partner Ssa Hsp70 isoforms.** The oncogene v-Src of the Rous sarcoma virus is one of the well-studied Hsp90 clients in the yeast *S. cerevisiae*. Although *S. cerevisiae* does not encode for v-Src kinase, its heterologous expression and subsequent maturation leads to tyrosine phosphorylation of many cellular proteins (BRUGGE *et al.* 1987). The uncontrolled phosphorylation activity induces cellular growth arrest in the yeast. The poor growth of the yeast cells upon v-Src overexpression is thus indicative of native folding and maturation of the kinase to its active form. We first confirmed v-Src mediated cellular growth arrest in a wt strain encoding all four cytosolic Ssa Hsp70 isoforms (Figure S1). To examine the role of different Ssa Hsp70 isoforms in Hsp90 chaperoning functions, we overexpressed v-Src from a galactose-inducible promoter in yeast strains that express only one of the desired isoforms in the absence of all four chromosomally encoded Hsp70s. To achieve similar expression levels of the expressed Ssa Hsp70s, all isoforms are expressed under the same native constitutive Ssa2 promoter. Figure 1 shows the growth phenotypes of cells harboring either empty plasmid (EV) or plasmid-encoding v-Src under a galactose-inducible promoter. In the absence of v-Src expression, all strains expressing individual Ssa Hsp70 isoforms grew similarly (Figure 1A and 1B). The v-Src overexpression in strains expressing Ssa1 (A1) or Ssa2 (A2) as the sole source of Hsp70 led to growth defects as is evident from their poor growth onto SGal solid media. Interestingly, cells overexpressing v-Src with Ssa3 (A3) or Ssa4 (A4) as the sole Ssa Hsp70 grew better than A1 or A2. The v-Src-mediated growth defects were further examined using spot dilution assays onto solid growth media (Figure 1C). As observed for the

primary transformants, the A1 and A2 strains show higher v-Src-mediated toxicity than strains expressing stress-inducible Ssa Hsp70s. Similar results were obtained when A1-A4 strains expressing v-Src were grown at 30°C for 72 h in liquid-selective growth media with dextrose (SD) or with galactose (SGal) as the carbon source (Figure 1C). As the A1-A4 strains are isogenic except for the presence of different Ssa Hsp70 isoforms, the data suggest that stress-inducible Ssa Hsp70s function differently than the constitutive isoforms in promoting maturation of Hsp90 substrate v-Src.

To examine whether the distinct effect of stress-inducible Hsp70s is specific to v-Src or is more general for other Hsp90 clients, we further explored the maturation of an another Hsp90 client, Ste11, in the A2 and A4 strains. The Ste11 kinase is required for the activation of Ste12, which regulates pheromone response elements (PRE). The Ste11 maturation is thus widely monitored by the activity of β-galactosidase expressed under the control of PRE. The plasmid-encoding *PRE*-lacZ was transformed into the A2 or A4 strains. The transformants were grown on liquid SD media until 1 $O.D._{600nm}$ and were treated with α-factor for induction of Ste11 expression. β-galactosidase activity was monitored as described in the Materials and Methods section. Compared to A2, the β-galactosidase activity was found to be lower in the A4 cells (Figure S2). These results suggest that, similar to v-Src, Ste11 maturation is also reduced in A4 cells.

**The reduction in v-Src toxicity is due to faster degradation of v-Src.** The above results show that strains with stress-inducible Ssa3 or Ssa4 as the sole Hsp70s reduce v-Src mediated toxicity. Furthermore, a comparison of the growth phenotypes of A3 versus A4 cells shows that v-Src overexpression is less detrimental in cells expressing Ssa4 than those expressing Ssa3. To further explore the mechanism of reduced v-Src toxicity, we used A2 and A4 as representative members

of constitutive and stress-inducible Hsp70 chaperones. v-Src kinase requires Hsp90 chaperone machinery to fold to the native state and if folding fails, the kinase is targeted for degradation (AN *et al.* 2000; KUNDRAT AND REGAN 2010). We thus examined v-Src abundances in the A2 and A4 strains to explore whether v-Src toxicity in the A4 strain is reduced due to a defect in its maturation. The cells expressing FLAG-tagged v-Src from a galactose-inducible promoter were grown in liquid growth media containing galactose for 12 h and the cellular lysate was then fractionated onto 12% SDS-PAGE before probing with the anti-FLAG antibody. As shown in Figure 2A, the v-Src expression was approximately 2-2.5 fold lower in A4 than in the A2 strain.

To examine whether the relatively reduced abundance of v-Src in the A4 strain is due to an effect of the galactose-inducible promoter, GFP was used as a reporter gene to monitor the strength of the GAL1 promoter in the A1-A4 strains. The gene encoding GFP was subcloned under the GAL1 promoter and its expression was monitored using immunoblot analysis with anti-GFP antibodies and with fluorescence microscopy. Both the immunoblot analysis with the anti-GFP antibody (Figure S3A) and fluorescence microscopy (Figure S3B) showed that the GFP levels are similar in the A1-A4 strains, thus suggesting that the galactose promoter strength remains independent of variations in the Hsp70 isoforms.

We further examined the degradation rates of v-Src in cells expressing Ssa2 or Ssa4 as the sole Ssa Hsp70 source. The cells were grown under inducible conditions for 12 h and were then shifted to repressible media to suppress v-Src expression. The abundances of preformed v-Src were then monitored at different time intervals (Figure 2B). As was observed, although even after 30 min of chase, there was no significant change in the v-Src levels in the A2 cells and more than 60% of v-Src was found to be degraded in the A4 cells. After approximately 90 min of growth in repressible media, most of the preformed v-Src was degraded in the A4 cells whereas

more than 50% of the v-Src was still present in the A2 cells. The enhanced degradation in the A4 strain is specific to v-Src as both GFP and other cellular proteins showed similar abundances in the A2 and A4 strains (Figure S4). Collectively, the above data suggest that v-Src degradation rates are higher in the A4 strain than in the A2 strain.

The constitutively active mature v-Src randomly phosphorylates most of the tyrosine-containing proteins of the yeast proteome (BRUGGE *et al.* 1987). To examine the tyrosine kinase activity of v-Src, cells harboring v-Src expression plasmid were grown in inducible growth media. The cells were then lysed and the lysate was immunoblotted with an anti-phosphotyrosine antibody. As expected, most of cellular proteins were detected with the anti-phosphotyrosine antibody (Figure 2C) but the phosphorylation levels varied between the A2 and A4 strains. Overall, the band intensity, which is a reflection of v-Src kinase activity, was found to be higher in the lysate obtained from the A2 cells than that obtained from the A4 cells, thus suggesting relatively higher v-Src maturation levels in cells expressing Ssa2 than Ssa4 as the sole Ssa Hsp70 source. Thus, the v-Src kinase activities in the A2 and A4 cells paralleled the growth defects observed in these strains. Overall, these results show that v-Src maturation is significantly reduced in strains expressing Ssa4 Hsp70 as the partner Hsp90 protein; these results indicate that different Hsp70 isoforms function differently in the Hsp90 chaperoning pathway.

**The A2 and A4 strains expressing v-Src show similar abundances of other major chaperones.** To explore whether the observed differences in v-Src maturation are related to altered abundances of the major heat shock proteins involved in client protein maturation, we examined the expression levels of Hsp70, Ydj1, Sse1, Hsp104 and Hsp90 in both the A2 and A4 strains. Both Ydj1 and Sse1 are known to affect v-Src maturation suggesting important role of both co-chaperones in Hsp90-dependent functions (DEY *et al.* 1996; GOECKELER *et al.* 2002).

Similarly, Hsp104 is known to interact with Hsp90 co-chaperones as well as with Hsp70 (ABBAS-TERKI *et al.* 2001; REIDY AND MASISON 2010).

We first examined the Ssa2 and Ssa4 levels in the A2 and A4 strains, respectively. Since the Hsp70 antibody recognizes Ssa2 with 3 times higher affinity than Ssa4 (GUPTA *et al.* 2018), the cellular abundances of the Ssa Hsp70 isoforms were measured by normalizing the amount of Hsp70 detected in the whole-cell lysate with respect to that observed using in vitro purified Hsp70s (Figure 3A). In agreement with our previous study, similar Ssa2 and Ssa4 levels were observed from A2 and A4 strains, respectively and suggest that the variations in kinase maturation are not due to varying Hsp70s levels.

To monitor Ydj1 abundances, the cellular lysates from the A2 and A4 cells were normalized for the total protein amount and were further probed onto immunoblot with antibodies against Ydj1 (Figure 3B). As seen in Figure 3B, Ydj1 was found to be similar in both the A2 and A4 strains. As v-Src is an Hsp90 substrate, we further examined Hsp90 abundances similar to those described above for Ydj1. We first examined the specificity of the anti-Hsp90 antibody for either of the two Hsp90 isoforms, namely, Hsc82 and Hsp82. As shown in Figure S5, the antibody detects both of the Hsp90 isoforms. The immunoblot results with the anti-Hsp90 antibodies showed that Hsp90 is expressed similarly in both the A2 and A4 strains (Figure 3B). Similarly, no significant differences were observed for Hsp104 and Sse1 in the A4 strain versus the A2 strain. These results generally suggest that decreased v-Src toxicity in the A4 strain is not related to altered levels of the major heat shock proteins.

**v-Src interaction with Ssa4 is lower than with Ssa2.** The reduced tyrosine phosphorylation activity and associated toxicity of v-Src in the A4 strain indicates a defect in its maturation to a native folded state. As v-Src is an Hsp90 substrate and this interaction facilitates v-Src

maturation, we conducted immunoprecipitation assays to examine the v-Src interactions with Hsp90 in both the A2 and A4 strains. Cells expressing FLAG-v-Src were grown for 12 h and the cellular lysates were incubated with immobilized beads of anti-FLAG antibodies. As the v-Src steady state level is lower in A4 cells, for immunoprecipitation studies greater quantities of cellular lysate from A4 cells (3X) were incubated with beads coated with anti-FLAG antibodies to capture equal amounts of v-Src from the A2 and A4 strains. The similar levels of immobilized v-Src were confirmed on immunoblot with anti-FLAG antibodies (Figure 4, upper panel). The co-immunoprecipitated proteins were further probed with the anti-Hsp90 antibody. As shown in Figure 4, although similar levels of v-Src were detected, more Hsp90 was obtained from A2 than from the A4 strain, thus suggesting that less of the v-Src interacts with Hsp90 in the A4 strain.

It is known that many Hsp90 substrates first interact with Hsp70 before being transferred to Hsp90 (ARLANDER *et al.* 2006; CINTRON AND TOFT 2006). To explore whether reduced levels of the v-Src-Hsp90 complex in the A4 strain are due to altered upstream interactions of v-Src with Hsp70s, we examined its interactions with Ssa2 and Ssa4. Similar to that described above for Hsp90, the co-immunoprecipitated proteins with FLAG-v-Src were further probed with anti-Hsp70 antibodies. As seen for Hsp90, although both Ssa2 and Ssa4 were detected at similar levels in the cellular lysates, less Ssa4 was found in the co-immunoprecipitated protein sample (Figure 4). These results suggest that although Ssa2 or Ssa4 are highly homologous, their binding properties with v-Src differ significantly in vivo.

**Both the Ssa2 and Ssa4 isoforms interact similarly with Hsp90.** We further examined the ability of Ssa2 and Ssa4 to interact with Hsp90. $His_6$-Hsp82 was used as the immobilized bait for the Hsp70s present in the cellular lysates from the A2 and A4 strains. Equal amounts of purified hexa-His tagged Hsp82 ($His_6$-Hsp82) were bound over a cobalt-based metal affinity resin. The

cellular lysates obtained from the A2 and A4 cells expressing FLAG-v-Src were passed through $His_6$-Hsp82 bound beads. The beads were subsequently washed and the bound proteins were eluted using 20 mM EDTA. The eluted proteins were then immunoblotted with anti-Hsp70, anti-Hsp90 and anti-FLAG tag antibodies. The eluted fractions from the A2 and A4 cellular lysates, when probed with the anti-Hsp70 antibody, showed similar levels of Hsp70s, thus suggesting that the two Hsp70 isoforms bind with similar affinities to Hsp90 (Figure 5). Furthermore, lower amounts of v-Src were found in the eluted fraction from A4 than in the eluted fraction with A2 cells; this result is in agreement with above data and shows that v-Src binds with lower affinity to Hsp90 in A4 (Figure 5). Overall, the above data show that both A2 and A4 bind with similar affinity to Hsp90 and A4 cells but less of the v-Src interacts with Hsp90 which could be due its relatively poor interaction with Ssa4 compared to that with Ssa2.

**Ydj1 interacts poorly with Ssa4 compared to Ssa2.** As Ydj1 is known to play an important role in substrate transfer to Hsp70s (DEY *et al.* 1996), we next explored the ability of v-Src to interact with Ydj1 in A2 and A4 cells expressing FLAG-tagged v-Src. The interactions were examined using a pull down assay with Ydj1 as the bait protein and the bound fractions were probed with anti-FLAG antibodies. As shown in Figure 6A, roughly similar amounts of v-Src were detected in the A2 and A4 strains, suggesting that Ydj1 binds with similar affinity to v-Src from either the A2 or A4 strain.

We next determined the interactions between Ydj1 and Ssa2 or Ssa4 using methods similar to those mentioned above for its interaction with v-Src. The eluted fractions from Ydj1 bound beads were probed with anti-Hsp70 or anti-Hsp90 antibodies. Figure 6A shows that compared to Ssa2, significantly lower amounts of Ssa4 were detected in the eluted fraction, thus suggesting

that Ydj1 binds with relatively weaker affinity to Ssa4 than to Ssa2. Interestingly, Hsp90 from the A2 and A4 cells was found to interact similarly with Ydj1.

To further examine the Ydj1 interactions with the Ssa Hsp70 isoforms, we conducted biolayer interferometry (BLI) studies with purified chaperones as described in the Materials and Methods section. Biolayer interferometry is an optical label-free method that is extensively used to monitor biomolecular interactions in real time. The Ydj1-loaded biosensor tips were immersed in solutions containing ATP (5 mM) and with increasing concentrations of one of the Hsp70 isoforms (Ssa2 or Ssa4). Figure 6B shows the sensorgrams for the binding of Ydj1 with the Ssa Hsp70 isoforms. As seen, incubation of the Ydj1-coated biosensor tips with solutions containing Ssa2 or Ssa4 led to increases in the BLI signals. The binding response increased with increasing concentrations of the Ssa Hsp70 isoforms. Furthermore, at similar concentrations, the binding response was much stronger for Ssa2 than for Ssa4 and suggests that the Ydj1 affinity is higher for Ssa2 than for Ssa4, which is in agreement with abovementioned pull down assays that showed relatively stronger binding of Ydj1 with Ssa2.

**Ydj1-assisted substrate refolding is more efficient with Ssa2 than with Ssa4.** As Ydj1 assists Hsp70 in stimulating ATPase activity as well as in substrate transfer, any variation in its interaction with Ssa2 versus Ssa4 might affect the downstream maturation of Hsp70 or Hsp90 substrates. We therefore further explored the Ydj1-assisted refolding of thermally denatured luciferase, which is a well-known Hsp70 substrate. Luciferase unfolds upon incubation at higher temperatures and its refolding back to a native state requires the presence of Hsp70. This refolding is further enhanced when Hsp90 is co-incubated with Hsp70s in a refolding buffer.

Luciferase was denatured by incubation at 45˚C for 10 min. Refolding was initiated by incubating denatured luciferase with Ydj1 in both the presence and absence of Ssa2 or Ssa4 at

25°C for different time intervals. As seen in Figure 7A, the presence of Ydj1 alone in the refolding buffer was not able to refold luciferase. As expected, the fraction of refolded luciferase, as measured by the increase in luminescence, increased when Ssa2 or Ssa4 was added into the refolding buffer containing Ydj1. The refolding level increased with increasing incubation time and saturated at approximately 30 min. Although luciferase refolded in the presence of either Ssa2 or Ssa4, the fraction of refolding was found to be significantly greater for Ssa2 than for Ssa4 (Figure 7A). After 30 min of incubation with Ssa2:Ydj1, the luciferase refolding level was approximately 25-fold, compared to only 2.5-fold with Ssa4:Ydj1. Overall the data suggest that the Ssa2:Ydj1 complex is more efficient than Ssa4:Ydj1 for the refolding of denatured luciferase. These results are in agreement with above pull down assay which showed weaker Ydj1 interaction with Ssa4 than with Ssa2.

We next examined the effect of Hsp90 on the refolding of denatured luciferase. The bridge protein Sti1 was added to the refolding reaction containing either Ssa2 or Ssa4 isoforms and Ydj1, and the refolding was monitored in both the presence and absence of an Hsp82 isoform of Hsp90. As expected, the addition of Hsp90 further enhanced luciferase refolding and relatively more so in reactions containing Ssa2 rather than Ssa4 (Figure 7B). After 30 min of incubation, the luciferase refolding was approximately 66-fold in the reaction containing Ssa2:Ydj:Sti:Hsp82, compared to a level of only 16-fold with Ssa4:Ydj1:Sti1:Hsp82. Overall, these studies suggest that Ydj1:Ssa2:Hsp90 has higher refolding activity than Ydj1:Ssa4:Hsp90.

The above results suggest that Ydj1 association with Ssa Hsp70 is crucial for substrate refolding. To confirm whether Ydj1 is also crucial for maturation of v-Src in vivo, we examined wt and *ydj1Δ* strains for v-Src mediated growth defects. The cells were transformed with the plasmid-encoding FLAG-v-Src under a galactose-inducible promoter and the transformants were further

monitored for growth onto media containing dextrose or galactose as the carbon source. As shown in Figure S6, in the presence of v-Src, cells lacking Ydj1 grew significantly more than wt cells, thus suggesting the critical role of Ydj1 in v-Src maturation.

**The functional distinction between Ssa2 and Ssa4 is governed by their C-terminal domains.** Ydj1 interacts with Hsp70 at ATPase as well as the C-terminal domain (GONG *et al.* 2018). Although Ydj1 interaction with the ATPase domain is crucial for stimulating Hsp70 ATPase activity, its coordination with the C-terminal domain facilitates substrate transfer (DEMAND *et al.* 1998).

To examine the role of NBD and CTD in determining the functional distinction of the Ssa Hsp70 isoforms, we swapped these domains and constructed two hybrid proteins based upon Ssa2 and Ssa4 as the parent proteins (Figure 8A). The hybrid Ssa24 encodes the NBD and SBD of Ssa2 and the CTD of Ssa4. Similarly, Ssa42 encodes the NBD and SBD of Ssa4 and the CTD of Ssa2. Strains expressing Ssa24 or Ssa42 (e.g., A24 or A42, respectively) as the sole Ssa Hsp70 source were constructed and examined for v-Src toxicity. In the absence of v-Src, the strains expressing the hybrid proteins showed similar growth on liquid YPAD as well as on solid SD media, thus suggesting that designed hybrid proteins are well folded and functionally active (Figure 8A and 8B). Furthermore, the hybrid proteins were expressed at similar levels as those of wt Ssa2 or Ssa4 (Figure S7). As seen before, the toxicity is reduced in the Ssa4 strain compared to Ssa2. For strains expressing hybrid proteins, we found that the v-Src overexpression was less toxic in strains expressing Ssa24 than in those expressing Ssa42 (Figure 8B); this result suggests that the C-terminal domain governs the functional distinction between Ssa2 and Ssa4 for the activities required for maturation of the Hsp90 client protein v-Src. The reduced toxicity of the Ssa24 strain is not due to an altered expression of other chaperones such as Ydj1 and Hsp90 and

suggests a direct role of the hybrid chaperone in maturation of v-Src kinase (Figure S7). v-Src maturation was further confirmed by measuring its steady state level in the Ssa24 and Ssa42 expressing strains. As shown in Figure 8C, the v-Src levels were found to be much lower in Ssa24 than in Ssa42; this result suggests its higher degradation in Ssa24. To further explore whether lower levels of v-Src in A4 and A24 are related to lower amounts of v-Src transcription, we conducted qRT-PCR with primers specific for v-Src. As shown in Figure 8D, no significant differences in v-Src mRNA levels were observed in A4 and A24 compared to A2 and A42, respectively.

We further measured the Ydj1 interactions with hybrid Ssa24 and Ssa42 using a pull down assay with $His_6$-tagged Ydj1 as the bait protein. The $His_6$-Ydj1 was bound over cobalt metal affinity beads and the cellular lysates from the A24 and A42 cells were passed through the Ydj1-bound beads (Figure S8). Similar to the results shown above, Ydj1 binds with relatively higher affinity to Ssa2 than to Ssa4. For the hybrids, the Ydj1 interaction with Ssa24 is stronger than with Ssa42, thus suggesting that the nucleotide binding domain plays a dominant role in regulating Ydj1 interactions with Ssa Hsp70; this is expected based on previous findings (JIANG *et al.* 2007).

Overall, these results point toward a role of the C-terminal domain of the Hsp70 isoforms in determining the functional distinction between Ssa2 and Ssa4 in the Hsp90 pathway.

**Discussion:**

Hsp70 and Hsp90 along with their co-chaperones form two major classes of cellular chaperone machinery. Hsp70-mediated substrate refolding is independent of Hsp90 actions, however Hsp90 requires Hsp70 for the maturation of many of its client proteins. Therefore, insight into how Hsp70 coordinates with Hsp90 is critical to further enhance our understanding of Hsp90

function. As eukaryotes carry multiple cytosolic members of the Hsp70 family, the role of each of these highly homologous members in Hsp90 activity is not clear. Although the members of the Hsp70 or Hsp90 families are very homologous within each family, they function distinctly in many cellular processes. The current study thus dissects the role of each of the Hsp70 isoforms in the Hsp90 pathway and shows that different isoforms behave differently with Hsp90s and that the distinction is primarily governed by the C-terminal domain of Hsp70s.

The results showing maturation of the Hsp90 clients v-Src and Ste11 in strains with different Ssa Hsp70 isoforms reveal clear distinctions between the roles of the constitutive and stress-inducible Hsp70s in the Hsp90 chaperoning pathway. The growth of A3 and A4 cells even with v-Src overexpression could either be due to a cytoprotective action of the stress-inducible Ssa Hsp70 isoforms or a lack of the function required for folding of the Hsp90 substrate to its active conformation that is critical for uncontrolled protein tyrosine phosphorylation. Several lines of evidence suggests that the lack v-Src folding protects cells from growth arrest. First, the level of protein phosphorylation is significantly lower in A4 than in the A2 strain and suggests reduced accumulations of active v-Src kinase. Second, the higher degradation rate of v-Src in A4 than in A2 cells is also an indication of its reduced maturation. Third, the wt strain expressing all four Ssa Hsp70 isoforms when grown under heat stress conditions is unable to reduce v-Src toxicity and suggests a recessive role for Ssa3 or Ssa4 with regard to v-Src associated toxicity (Figure S9). These results thus suggest that constitutively expressed Ssa Hsp70s cooperate better than their stress-inducible members with Hsp90s for folding of its client proteins. It is likely that the evolutionary pressure on Hsp70s to coordinate with Hsp90s might have been more selective toward the constitutively present Ssa Hsp70s rather than for those isoforms that are expressed only under stress. These results thus suggest that in addition to their redundant roles, the

388 constitutive and stress-inducible Hsp70 members are also evolved with more specialized distinct
389 functions such as their role in the Hsp90 pathway. This agrees with our previous results showing
390 that A3 cells more effectively reduce α-synuclein toxicity than A2 cells; this cytoprotective
391 effect is primarily mediated through autophagy (GUPTA *et al.* 2018).

392 Hsp90 coordinates with Hsp70 for many of its cellular functions. Interaction studies using
393 immunoprecipitation of FLAG-v-Src have revealed that the client interacts poorly with Hsp90s
394 in A4 compared to the A2 strain. Since the same Hsp90 isoforms are present in the A2 and A4
395 strains, it is intriguing to note that the v-Src interaction with Hsp90 is strain-dependent. Both the
396 A2 and A4 strains are isogenic, except for the presence of Ssa2 and Ssa4, respectively and thus
397 the distinct v-Src-Hsp90 interactions must be regulated by the Hsp70 isoforms or their
398 interacting co-chaperones. The Hsp70 interactions with Hsp90 are known to be mediated through
399 nucleotide binding domain as well as EEVD motif present at the C-terminus of these proteins
400 (KRAVATS *et al.* 2017). Our results from the pull down assay show that both Ssa2 and Ssa4
401 interact similarly with Hsp82, and thus the relatively weaker interaction of v-Src with Hsp82 in
402 the A4 strain might be due to a cellular process upstream of the Hsp70-Hsp90 collaboration.

403 Next, we find that the v-Src interaction with Ssa4 is relatively weaker than the interaction with
404 Ssa2, which could be the basis for the relatively poor interaction observed between v-Src and
405 Hsp90 in the A4 strain. Similar to other known substrates, v-Src could interact with Hsp70s
406 either directly or through the Hsp70 co-chaperone Ydj1 (DEY *et al.* 1996). The pull down study
407 using $His_6$-tagged Ydj1 shows that the co-chaperone interaction with v-Src is similar in both the
408 A2 and A4 strains. Furthermore, the pull down study revealed that the Ydj1 interaction with Ssa2
409 is stronger than with Ssa4. The weaker interaction of Ydj1 with Ssa4 was further confirmed
410 using purified chaperones in vitro. The relatively weaker interaction of Ydj1 with Ssa4 is in

agreement with the lower luciferase refolding activity seen in the reactions containing Ydj1 and Ssa4 instead of Ssa2. Ssa2 was able to promote luciferase refolding at levels 25-30 times greater than for Ssa4. Similarly, higher activity was observed with Ssa2 than with Ssa4 when luciferase refolding assays were carried out in the presence of Hsp82 with either of the Hsp70 isoforms and Ydj1. This study generally reveals a novel distinction in the interactions of Ydj1 with Ssa2 versus the interactions with Ssa4. As the Ssa4 interaction with Ydj1 is relatively weaker, it is possible that this leads to poor substrate transfer from Ydj1 to Ssa4, resulting in lower abundances of v-Src-Ssa4 complex as observed in the immunoprecipitated complex against v-Src.

Hsp40 proteins are known to interact at the NBD (JIANG *et al.* 2007) or the CTD of Hsp70 (DEMAND *et al.* 1998; GONG *et al.* 2018) , and influence Hsp70 function (SLUDER *et al.* 2018). The CTDs of Ssa2 and Ssa4 are more divergent (i.e., a sequence identity of 42%) than their NBDs (i.e., a sequence identity of 87%). The interaction of Ydj1 with NBD stimulates the ATPase activity of Hsp70 (LAUFEN *et al.* 1999; JIANG *et al.* 2007) whereas those at the CTD are known to facilitate substrate transfer (FREEMAN *et al.* 1995; DEMAND *et al.* 1998). The pull down assay shows that the Ydj1 interaction with Ssa24 is stronger than it is with Ssa42 and suggests that the Ydj1-Ssa interaction is primarily mediated by the N-terminal domain. Our study used the hybrid Ssa chaperones Ssa24 and Ssa42, showing that cells expressing Ssa24 reduce v-Src toxicity better than those expressing Ssa42 and reveals that the C-terminal domain mediates the functional distinction of Ssa proteins in the Hsp90 chaperoning pathway. It is possible that, although Ydj1 interacts strongly with Ssa24 through its N-terminal domain, its interaction with the less-conserved CTD of Ssa4 remains compromised and results in poor v-Src transfer to the hybrid Ssa Hsp70 and leads to relatively lower maturation of the kinase. This is in agreement

with lower abundance of the v-Src-Ssa4 complex in the A4 strain (Figure 4) although Ydj1 interacts similarly with v-Src in both the A2 and A4 strains. Our results suggest that although the N-terminal domain of Hsp70 governs its interaction with Ydj1, the C-terminal domain determines the functional specificity between Ssa2 and Ssa4 with respect to v-Src toxicity.

The pull down experiments using Ydj1 further reveal its interaction with Hsp90. The Ydj1 interaction with Hsp90 could either be direct or indirect through Hsp70. Since Ydj1 shows similar interactions with Hsp90 in spite of the different affinities toward the Ssa Hsp70 isoforms, the interaction of Ydj1 with Hsp90 (as seen in the pull down assay) is more likely to be a direct interaction. Furthermore, as Ydj1 interacts similarly with Hsp90 in the A2 and A4 strains, the distinct v-Src activity and related toxicity might not be due to any activity associated with the formation of the Ydj1-Hsp90 complex in these strains.

In summary, our data suggest that v-Src interacts similarly with Ydj1 in the A2 and A4 strains but that the client transfer from Ydj1 to Hsp70 is less efficient for Ssa4 than for Ssa2. The lack of v-Src-Ssa4 interaction leads to substrate inactivation and degradation. In contrast, v-Src is transferred efficiently to Ssa2. Hsp90 then interacts with v-Src and promotes its maturation to active kinase (Figure 9).

Hsp70s are involved in a variety of cellular functions. Although different Hsp70 isoforms perform many redundant functions, functional distinctions among these are also known. What governs the functional specificity among highly homologous Hsp70s is not clear and the role of the co-chaperones is generally believed to the underlying basis of specificity. The current study shows that different Ssa Hsp70 isoforms function distinctly in the Hsp90 chaperoning functions. Interestingly, the functional distinctions of the Ssa Hsp70 isoforms lie upstream of their interactions with the co-chaperone Ydj1. The results provided here thus show that Hsp40s are

not only required to activate the Hsp70 reaction cycle but also influence its function and thus provide functional diversity within members of the Hsp70 family.

## Materials and Methods

### Strains and Plasmids

The strains & plasmids used in the study are described in Table 1 and 2 respectively.

Plasmid pRS316$P_{GAL1}$-GFP is a URA3-based single copy vector with *GFP* under GAL1 promoter. For protein purification, *HSP82* and *STI1* were subcloned into pET29bHTV plasmid using PCR based amplification of respective genes and further digestion using BamH1 and Xho1 to generate pET29bHTV-HSP82 and pET29bHTV-STI. The plasmid encodes from 5' to 3' direction, a Hexa-His-tag, a TEV protease recognition site and *HSP82* or *STI1*.

### Media and Growth conditions

Media composition is as described before (KUMAR *et al.* 2014). Synthetic-defined (SD) media is composed of yeast nitrogen base (YNB) (BD-233520) with ammonium sulfate (0.67%) and 2% dextrose (Fisher-50-99-7). SGal media is similar to SD media except it was supplemented with 2% Raffinose (Sigma-R0250) and 2% Galactose (Sigma-G0625) instead of dextrose. YPAD media is composed of 1% yeast extract (BD-212750), 2% peptone (BD-244620) and 2% dextrose supplemented with 0.005% adenine (Sigma-A9126). Cells were grown at 30°C unless specifically mentioned. Amino acids were supplemented as required.

### Immunoblot analysis:

Cells grown in liquid media were harvested by centrifugation, and lysed using glass beads. The lysate was further fractionated into supernatant and pellet. The proteins separated on SDS-PAGE were transferred onto polyvinylidene fluoride (PVDF) membranes, and further probed using desired antibodies. The primary antibodies used in the study are obtained as follows: anti-FLAG

antibody (F3165 Sigma), anti-Phosphotyrosine (05-321 Millipore), Anti-GFP (MA5-15256 Thermo Scientific), anti-Sse1 (A kind gift from Dr. Brodsky), anti-Ydj1 (SAB5200007 Sigma), anti-Hsc82 (ab30920 Abcam), anti-Hsp70 (ADI-SPA-822-F Enzo Lifesciences), and anti-Pgk1 (catalog number 459250 Invitrogen). Primary antibodies were used at dilution of 1:5000, and incubated with immunoblot for 1h at 25°C. Lysate for A4 was loaded 3 times (3X) of A2 lysate to correct for lower v-Src level in A4 strain, and also for lower anti-Hsp70 antibody affinity for Ssa4 than Ssa2.

Densitometric analysis of immunoblots was performed using UN-SCAN-IT software.

**Chase experiments:**

Yeast strains were grown in selective liquid SD media at 30°C until $O.D._{600nm}$ reaches 0.8-1. Cells were collected using centrifugation and washed 3 times with sterile water. The v-Src expression was induced by diluting cells into selective liquid SGal media to 0.5 $O.D._{600nm}$. Cells were further grown for 12 hours at 30°C. Galactose mediated protein expression was terminated by shifting cells to growth media containing dextrose instead of galactose. To monitor v-Src degradation, the culture aliquots were collected at mentioned time points. Cells were harvested, and lysed using mechanical disruption. The cellular lysate was further probed on immunoblot using anti-FLAG antibody (F3165 Sigma).

**Protein Purification:**

Ydj1 was purified as described earlier (SHARMA AND MASISON 2011).

For Hsp82 and Sti1 purification plasmids pET29bHTV-HSP82 and pET29bHTV-STI1 were transformed in *E.coli* Rosetta DE3 (Invitrogen) strains. Culture was grown in Luria Broth until 0.7 $O.D._{600nm}$ and protein expression was induced with 0.3mM IPTG at 37°C for 3 hours. Cells were lysed, and $His_6$-tagged Hsp82 was purified from cellular lysate through cobalt based Talon

metal affinity resin. To remove $His_6$-tag, purified $His_6$-Hsp82 was incubated with $His_6$-TEV. The cleaved $His_6$-tag along with TEV protease recognition site and $His_6$-TEV protease was further removed using metal affinity column.

Sti1 was purified using process similar to as described above for Hsp82.

Ssa2 and Ssa4 were purified similar to the process described before for Ssa2 (GUPTA *et al.* 2018). Briefly, strains harboring plasmid pRS416$P_{GPD}$-$His_6$SSA2 or pRS416$P_{GPD}$-$His_6$SSA4 as sole source of Ssa Hsp70 were grown in liquid YPAD media for 24 hours at 30°C. Cells were harvested and re-suspended in 20 mM HEPES, 150 mM NaCl, 20 mM KCl and 20 mM $MgCl_2$, pH 7.4 buffer (Buffer A) containing protease inhibitor cocktail (Pierce).Cell lysis was carried out using glass beads followed by sonication. Protein purification was carried out using cobalt based metal affinity resin. The N-terminal $His_6$ tag was removed using TEV protease as described above for Hsp82. The $His_6$ tag cleaved purified protein was further incubated with ATP-Agarose resin for 4 hours and eluted with buffer A containing 7 mM ATP and 1 mM DTT (GUPTA *et al.* 2018). Protein purity was confirmed on 10% SDS-PAGE.

The hybrid proteins, Ssa24 and Ssa42 were purified similar to as described above for Ssa2.

**Immunoprecipitaion and Pull down:**

For immunoprecipitation study, cells were resuspended in 20 mM Tris pH 7.5 buffer containing 150 mM NaCl, 0.5 mM EDTA and 1 mM PMSF, and lysed by mechanical disruption using glass beads. The lysate was incubated overnight with anti-FLAG antibody attached resin (Sigma A220). The unbound fraction in supernatant was removed by centrifugation at 4000g for 1 min. The beads were washed with buffer containing 150 mM NaCl, 0.1% Triton X-100, and 20 mM Tris pH 7.5, and immunoprecipitated proteins were further analyzed on immunoblot using various antibodies.

The pull down studies were performed as described earlier (KUMAR *et al.* 2015). Briefly, purified $His_6$-Ydj1 or $His_6$-Hsp82 were bound to cobalt based affinity resin, followed by incubation with yeast lysate. The resin was further washed to remove unbound proteins. Bound fraction was eluted using 20 mM EDTA and probed with desired antibodies.

**Quantitative Real-Time PCR:**

The cells were harvested and total RNA was purified using HiPurA Yeast RNA Purification Kit (MB611 from HiMedia) following manufacturer's protocol. About 100ng of isolated RNA was used to prepare cDNA using cDNA synthesis kit (Verso from Thermo Scientific AB1453B). 50 ng of cDNA was used as template for quantitative Real-Time PCR (qRT-PCR) using DyNAmoColorFlash SYBR green PCR kit (Thermo scientific FNZ416L) on Steponeplus™ Real time PCR system (Applied Biosystems).

**Luciferase refolding assay:**

Luciferase refolding assay was carried out similar to the procedure described before (KRAVATS *et al.* 2018) with few modifications. Briefly firefly luciferase (80 nM) from Promega was denatured in the presence of 1 mM ATP at 45°C for 10 min. The denatured luciferase (40 nM) was refolded in presence of 0.3 μM Ydj1 with or without 0.5 μM Hsp70 (Ssa2 or Ssa4). The reaction was incubated at 25°C, and refolding was initiated by addition of 1 mM ATP. The refolding was measured as increase in luminescence with time. To examine the effect of Hsp90 on luciferase refolding, denatured luciferase (40 nM) was incubated in the presence of 0.3 μM Ydj1, 0.5 μM Hsp70 (Ssa2 or Ssa4), 2.4 μM Sti1 and 0.9 μM Hsp82, and the refolding was monitored as stated above.

**Ste11 kinase assay:**

Yeast cells were transformed with plasmid PRE-lacZ having lacZ gene driven by pheromone response elements (MORANO AND THIELE 1999). The cells were grown until 1 $O.D._{600nm}$ and further treated with α-factor (5 μM) for 6 hours. The β-galactosidase activity was measured as described before (MORANO AND THIELE 1999). Briefly, 1 $O.D._{600nm}$ cells were permeabilized using freeze thaw method. The cells were incubated with 200μl of ONPG (4 mg/ml) for 15 min followed by addition on 1 M $Na_2CO_3$. The cells were separated using centrifugation, and supernatant was used for measuring absorbance at 420nm.

**Biolayer Interferometry:**

The Biolayer Interferometry studies were performed using Octet K2 instrument (ForteBio) to monitor interaction between Ydj1 with different Hsp70 isoforms at 30°C. The Ydj1 was immobilized on amine reactive second generation (AR2G) biosensors, activated using 1:1 ratio of 0.1M N-Hydroxysuccinimide (NHS) and 0.4M 1-ethyl-3-(3-dimethylaminopropyl)-carbodiimide (EDC), to response signal of 1nm. Post immobilization, the biosensor was blocked with 1M ethanolamine. The reference biosensor was activated similarly except assay buffer (25 mM HEPES pH 7.4, 150 mM NaCl, 20 mM $MgCl_2$ and 20 mM KCl) lacking Ydj1 was used for immobilization on AR2G biosensors. The Ydj1 immobilized and reference biosensors were dipped into assay buffer containing increasing concentrations (0.2 5μM to 1 μM) of Ssa Hsp70 isoforms in a 96 well plate, and binding was monitored as increase in binding response for 200s. Dissociation was monitored in buffer alone for 200s. The non-specific signal obtained from reference biosensor was subtracted from corresponding response signal of Ydj1 and Hsp70 interaction. The obtained binding sensorgrams were analyzed using software 'Data Analysis 9.0' available from ForteBio.

**Significance test:**

Three biological replicates were performed for each experiment. To compare significance among the groups student's *t*-test was used. The p values are shown as follows: * $p < 0.05$, ** $p < 0.01$, *** $p < 0.001$, with a $p < 0.05$ considered statistically significant.

**Data availability statement:**

Strains and plasmids are available upon request. The authors affirm that all data necessary for confirming the conclusions of the article are present within the article, figures, and tables. Supplemental material at https://doi.org/10.25386/genetics.12136941 .

**Acknowledgments:**

We thank Dr. Daniel Masison for critical reading of the manuscript. We thank Prof. Kevin Morano for providing PRE-lacZ plasmid as a kind gift. We also thank Prof. Jeffrey Brodsky for providing anti-Sse1 antibody as a kind gift.

## References:

Abbas-Terki, T., O. Donzé, P. A. Briand and D. Picard, 2001 Hsp104 interacts with Hsp90 cochaperones in respiring yeast. Molecular and cellular biology 21**:** 7569-7575.

An, W. G., T. W. Schulte and L. M. Neckers, 2000 The Heat Shock Protein 90 Antagonist Geldanamycin Alters Chaperone Association with p210bcr-abl and v-src Proteins before Their Degradation by the Proteasome. Cell Growth Differentiation 11**:** 355-360.

Arlander, S. J. H., S. J. Felts, J. M. Wagner, B. Stensgard, D. O. Toft *et al.*, 2006 Chaperoning Checkpoint Kinase 1 (Chk1), an Hsp90 Client, with Purified Chaperones. Journal of Biological Chemistry 281**:** 2989-2998.

Boysen, M., R. Kityk and M. P. Mayer, 2019 Hsp70- and Hsp90-Mediated Regulation of the Conformation of p53 DNA Binding Domain and p53 Cancer Variants. Molecular Cell 74**:** 831-843.e834.

Brugge, J. S., G. Jarosik, J. Andersen, A. Queral-Lustig, M. Fedor-Chaiken *et al.*, 1987 Expression of Rous sarcoma virus transforming protein pp60v-src in Saccharomyces cerevisiae cells. Molecular and cellular biology 7**:** 2180-2187.

Chang, H. C., D. F. Nathan and S. Lindquist, 1997 In vivo analysis of the Hsp90 cochaperone Sti1 (p60). Molecular and cellular biology 17**:** 318-325.

Chen, B., D. Zhong and A. Monteiro, 2006 Comparative genomics and evolution of the HSP90 family of genes across all kingdoms of organisms. BMC genomics 7**:** 156-156.

Cintron, N. S., and D. Toft, 2006 Defining the Requirements for Hsp40 and Hsp70 in the Hsp90 Chaperone Pathway. Journal of Biological Chemistry 281**:** 26235-26244.

Citri, A., D. Harari, G. Shohat, P. Ramakrishnan, J. Gan *et al.*, 2006 Hsp90 Recognizes a Common Surface on Client Kinases. Journal of Biological Chemistry 281**:** 14361-14369.

Dahiya, V., G. Agam, J. Lawatscheck, D. A. Rutz, D. C. Lamb *et al.*, 2019 Coordinated Conformational Processing of the Tumor Suppressor Protein p53 by the Hsp70 and Hsp90 Chaperone Machineries. Molecular Cell 74**:** 816-830.e817.

Demand, J., J. Lüders and J. Höhfeld, 1998 The carboxy-terminal domain of Hsc70 provides binding sites for a distinct set of chaperone cofactors. Molecular and cellular biology 18**:** 2023-2028.

Dey, B., A. J. Caplan and F. Boschelli, 1996 The Ydj1 molecular chaperone facilitates formation of active p60v-src in yeast. Molecular biology of the cell 7**:** 91-100.

Duina, A. A., H.-C. J. Chang, J. A. Marsh, S. Lindquist and R. F. Gaber, 1996 A Cyclophilin Function in Hsp90-Dependent Signal Transduction. Science 274**:** 1713.

Flower, T. R., L. S. Chesnokova, C. A. Froelich, C. Dixon and S. N. Witt, 2005 Heat Shock Prevents Alpha-synuclein-induced Apoptosis in a Yeast Model of Parkinson's Disease. Journal of Molecular Biology 351**:** 1081-1100.

Freeman, B. C., M. P. Myers, R. Schumacher and R. I. Morimoto, 1995 Identification of a regulatory motif in Hsp70 that affects ATPase activity, substrate binding and interaction with HDJ-1. The EMBO journal 14**:** 2281-2292.

Goeckeler, J. L., A. Stephens, P. Lee, A. J. Caplan and J. L. Brodsky, 2002 Overexpression of yeast Hsp110 homolog Sse1p suppresses ydj1-151 thermosensitivity and restores Hsp90-dependent activity. Molecular biology of the cell 13**:** 2760-2770.

Gong, W., W. Hu, L. Xu, H. Wu, S. Wu *et al.*, 2018 The C-terminal GGAP motif of Hsp70 mediates substrate recognition and stress response in yeast. Journal of Biological Chemistry 293**:** 17663-17675.

Graf, C., M. Stankiewicz, G. Kramer and M. P. Mayer, 2009 Spatially and kinetically resolved changes in the conformational dynamics of the Hsp90 chaperone machine. The EMBO journal 28**:** 602-613.

Gupta, A., A. Puri, P. Singh, S. Sonam, R. Pandey *et al.*, 2018 The yeast stress inducible Ssa Hsp70 reduces α-synuclein toxicity by promoting its degradation through autophagy. PLoS genetics 14**:** e1007751-e1007751.

Jiang, J., E. G. Maes, A. B. Taylor, L. Wang, A. P. Hinck *et al.*, 2007 Structural basis of J cochaperone binding and regulation of Hsp70. Molecular cell 28**:** 422-433.

Karagöz, G. E., A. M. S. Duarte, E. Akoury, H. Ippel, J. Biernat *et al.*, 2014 Hsp90-Tau complex reveals molecular basis for specificity in chaperone action. Cell 156**:** 963-974.

Kim, R. H., R. Kim, W. Chen, S. Hu, K.-H. Shin *et al.*, 2008 Association of hsp90 to the hTERT promoter is necessary for hTERT expression in human oral cancer cells. Carcinogenesis 29**:** 2425-2431.

Kirschke, E., D. Goswami, D. Southworth, P. R. Griffin and D. A. Agard, 2014 Glucocorticoid receptor function regulated by coordinated action of the Hsp90 and Hsp70 chaperone cycles. Cell 157**:** 1685-1697.

Kravats, A. N., S. M. Doyle, J. R. Hoskins, O. Genest, E. Doody *et al.*, 2017 Interaction of E. coli Hsp90 with DnaK Involves the DnaJ Binding Region of DnaK. Journal of Molecular Biology 429**:** 858-872.

Kravats, A. N., J. R. Hoskins, M. Reidy, J. L. Johnson, S. M. Doyle *et al.*, 2018 Functional and physical interaction between yeast Hsp90 and Hsp70. Proceedings of the National Academy of Sciences of the United States of America 115**:** E2210-E2219.

Kumar, N., D. Gaur, A. Gupta, A. Puri and D. Sharma, 2015 Hsp90-Associated Immunophilin Homolog Cpr7 Is Required for the Mitotic Stability of [URE3] Prion in Saccharomyces cerevisiae. PLoS genetics 11**:** e1005567-e1005567.

Kumar, N., D. Gaur, D. C. Masison and D. Sharma, 2014 The BAG homology domain of Snl1 cures yeast prion [URE3] through regulation of Hsp70 chaperones. G3 (Bethesda, Md.) 4**:** 461-470.

Kundrat, L., and L. Regan, 2010 Balance between folding and degradation for Hsp90-dependent client proteins: a key role for CHIP. Biochemistry 49**:** 7428-7438.

Laufen, T., M. P. Mayer, C. Beisel, D. Klostermeier, A. Mogk *et al.*, 1999 Mechanism of regulation of hsp70 chaperones by DnaJ cochaperones. Proceedings of the National Academy of Sciences of the United States of America 96**:** 5452-5457.

Leu, J. I. J., J. Pimkina, P. Pandey, M. E. Murphy and D. L. George, 2011 HSP70 inhibition by the small-molecule 2-phenylethynesulfonamide impairs protein clearance pathways in tumor cells. Molecular cancer research : MCR 9**:** 936-947.

Li, J., J. Soroka and J. Buchner, 2012 The Hsp90 chaperone machinery: Conformational dynamics and regulation by co-chaperones. Biochimica et Biophysica Acta (BBA) - Molecular Cell Research 1823**:** 624-635.

Lotz, S. K., L. E. Knighton, Nitika, G. W. Jones and A. W. Truman, 2019 Not quite the SSAme: unique roles for the yeast cytosolic Hsp70s. Current Genetics 65**:** 1127-1134.

Mayr, C., K. Richter, H. Lilie and J. Buchner, 2000 Cpr6 and Cpr7, Two Closely Related Hsp90-associated Immunophilins from Saccharomyces cerevisiae, Differ in Their Functional Properties. Journal of Biological Chemistry 275**:** 34140-34146.

McLaughlin, S. H., F. Sobott, Z.-p. Yao, W. Zhang, P. R. Nielsen *et al.*, 2006 The Co-chaperone p23 Arrests the Hsp90 ATPase Cycle to Trap Client Proteins. Journal of Molecular Biology 356**:** 746-758.

Minami, Y., Y. Kimura, H. Kawasaki, K. Suzuki and I. Yahara, 1994 The carboxy-terminal region of mammalian HSP90 is required for its dimerization and function in vivo. Molecular and Cellular Biology 14**:** 1459.

Morano, K. A., and D. J. Thiele, 1999 The Sch9 protein kinase regulates Hsp90 chaperone complex signal transduction activity in vivo. The EMBO Journal 18**:** 5953-5962.

Panaretou, B., G. Siligardi, P. Meyer, A. Maloney, J. K. Sullivan *et al.*, 2002 Activation of the ATPase Activity of Hsp90 by the Stress-Regulated Cochaperone Aha1. Molecular Cell 10**:** 1307-1318.

Picard, D., B. Khursheed, M. J. Garabedian, M. G. Fortin, S. Lindquist *et al.*, 1990 Reduced levels of hsp90 compromise steroid receptor action in vivo. Nature 348**:** 166-168.

Prodromou, C., G. Siligardi, R. O'Brien, D. N. Woolfson, L. Regan *et al.*, 1999 Regulation of Hsp90 ATPase activity by tetratricopeptide repeat (TPR)-domain co-chaperones. The EMBO journal 18**:** 754-762.

Rajapandi, T., L. E. Greene and E. Eisenberg, 2000 The Molecular Chaperones Hsp90 and Hsc70 Are Both Necessary and Sufficient to Activate Hormone Binding by Glucocorticoid Receptor. Journal of Biological Chemistry 275**:** 22597-22604.

Reidy, M., and D. C. Masison, 2010 Sti1 regulation of Hsp70 and Hsp90 is critical for curing of Saccharomyces cerevisiae [PSI+] prions by Hsp104. Molecular and cellular biology 30**:** 3542-3552.

Rodina, A., P. D. Patel, Y. Kang, Y. Patel, I. Baaklini *et al.*, 2013 Identification of an allosteric pocket on human hsp70 reveals a mode of inhibition of this therapeutically important protein. Chemistry & biology 20**:** 1469-1480.

Röhl, A., D. Wengler, T. Madl, S. Lagleder, F. Tippel *et al.*, 2015 Hsp90 regulates the dynamics of its cochaperone Sti1 and the transfer of Hsp70 between modules. Nature Communications 6**:** 6655.

Roy, J., S. Mitra, K. Sengupta and A. K. Mandal, 2015 Hsp70 clears misfolded kinases that partitioned into distinct quality-control compartments. Molecular biology of the cell 26**:** 1583-1600.

Sato, S., N. Fujita and T. Tsuruo, 2000 Modulation of Akt kinase activity by binding to Hsp90. Proceedings of the National Academy of Sciences 97**:** 10832.

Schmid, A. B., S. Lagleder, M. A. Gräwert, A. Röhl, F. Hagn *et al.*, 2012 The architecture of functional modules in the Hsp90 co-chaperone Sti1/Hop. The EMBO journal 31**:** 1506-1517.

Sharma, D., and D. C. Masison, 2008 Functionally redundant isoforms of a yeast Hsp70 chaperone subfamily have different antiprion effects. Genetics 179**:** 1301-1311.

699 Sharma, D., and D. C. Masison, 2011 Single methyl group determines prion propagation and protein
700 degradation activities of yeast heat shock protein (Hsp)-70 chaperones Ssa1p and Ssa2p.
701 Proceedings of the National Academy of Sciences of the United States of America 108**:** 13665-
702 13670.
703 Sluder, I. T., Nitika, L. E. Knighton and A. W. Truman, 2018 The Hsp70 co-chaperone Ydj1/HDJ2 regulates
704 ribonucleotide reductase activity. PLoS genetics 14**:** e1007462-e1007462.
705 Srisutthisamphan, K., K. Jirakanwisal, S. Ramphan, N. Tongluan, A. Kuadkitkan *et al.*, 2018 Hsp90
706 interacts with multiple dengue virus 2 proteins. Scientific Reports 8**:** 4308.
707 Sullivan, W. P., B. A. L. Owen and D. O. Toft, 2002 The Influence of ATP and p23 on the Conformation of
708 hsp90. Journal of Biological Chemistry 277**:** 45942-45948.
709 Taipale, M., I. Krykbaeva, M. Koeva, C. Kayatekin, K. D. Westover *et al.*, 2012 Quantitative analysis of
710 HSP90-client interactions reveals principles of substrate recognition. Cell 150**:** 987-1001.
711 Tibor Roberts, B., H. Moriyama and R. B. Wickner, 2004 [URE3] prion propagation is abolished by a
712 mutation of the primary cytosolic Hsp70 of budding yeast. Yeast 21**:** 107-117.
713 Voss, A. K., T. Thomas and P. Gruss, 2000 Mice lacking HSP90beta fail to develop a placental labyrinth.
714 Development 127**:** 1.
715 Warth, R., P. A. Briand and D. Picard, 1997 Functional analysis of the yeast 40 kDa cyclophilin Cyp40 and
716 its role for viability and steroid receptor regulation. Biological chemistry 378**:** 381-391.
717 Werner-Washburne, M., J. Becker, J. Kosic-Smithers and E. A. Craig, 1989 Yeast Hsp70 RNA levels vary in
718 response to the physiological status of the cell. Journal of bacteriology 171**:** 2680-2688.
719 Werner-Washburne, M., D. E. Stone and E. A. Craig, 1987 Complex interactions among members of an
720 essential subfamily of hsp70 genes in Saccharomyces cerevisiae. Molecular and cellular biology
721 7**:** 2568-2577.
722 Xu, Y., M. A. Singer and S. Lindquist, 1999 Maturation of the tyrosine kinase c-src as a kinase and as a
723 substrate depends on the molecular chaperone Hsp90. Proceedings of the National Academy of
724 Sciences of the United States of America 96**:** 109-114.

725

726

727 **Table1: List of strains used in the present study**

| Strain | Genotype | Reference |
|---|---|---|
| **SY187** | *MATa, kar 1-1, $P_{DAL5}$::ADE2, his3Δ202, leu2Δ1, trp1Δ63, ura3-52* | (SHARMA AND MASISON 2011) |
| **SY135** | *MATa, $P_{DAL5}$::ADE2, ssa1::Kan, ssa2::HIS3, ssa3::TRP1, ssa4::ura3-2f /pRS315$P_{SSA2}$-SSA1* | (SHARMA AND MASISON 2008) |
| **SY136** | *MATa, $P_{DAL5}$::ADE2, ssa1::Kan, ssa2::HIS3, ssa3::TRP1, ssa4::ura3-2f /pRS315$P_{SSA2}$-SSA2* | (SHARMA AND MASISON 2008) |
| **SY143** | *MATa, $P_{DAL5}$::ADE2, ssa1::Kan, ssa2::HIS3, ssa3::TRP1, ssa4::ura3-2f /pRS315$P_{SSA2}$-SSA3* | (SHARMA AND MASISON 2008) |
| **SY211** | *MATa, $P_{DAL5}$::ADE2, ssa1::Kan, ssa2::HIS3, ssa3::TRP1, ssa4::ura3-2f /pRS315$P_{SSA2}$-SSA4* | (SHARMA AND MASISON 2008) |
| **A42** | *MATa, $P_{DAL5}$::ADE2, ssa1::Kan, ssa2::HIS3, ssa3::TRP1, ssa4::ura3-2f /pRS315$P_{SSA2}$-SSA42* | This study |
| **A24** | *MATa, $P_{DAL5}$::ADE2, ssa1::Kan, ssa2::HIS3, ssa3::TRP1, ssa4::ura3-2f /pRS315$P_{SSA2}$-SSA24* | This study |
| **Asc200** | *MATa, $P_{DAL5}$::ADE2, ssa1::Kan, ssa2::HIS3, ssa3::TRP1, ssa4::ura3-2f /pRS416$P_{GPD}$-$His_6$SSA2* | (GUPTA *et al.* 2018) |
| **Asc400** | *MATa, $P_{DAL5}$::ADE2, ssa1::Kan, ssa2::HIS3, ssa3::TRP1, ssa4::ura3-2f /pRS416$P_{GPD}$-$His_6$SSA4* | (GUPTA *et al.* 2018) |

728

729

730 **Table 2: List of plasmids used in the present study**

| Plasmid | Marker | Reference |
|---|---|---|
| **pRS316P$_{GAL1}$-FLAG-vSrc** | URA3 | This study |
| **pRS316P$_{GAL1}$-GFP** | URA3 | This study |
| **PRE-lacZ** | URA3 | (MORANO AND THIELE 1999) |
| **pRS315P$_{SSA2}$-SSA1** | LEU2 | (SHARMA AND MASISON 2008) |
| **pRS315P$_{SSA2}$-SSA2** | LEU2 | (SHARMA AND MASISON 2008) |
| **pRS315P$_{SSA2}$-SSA3** | LEU2 | (SHARMA AND MASISON 2008) |
| **pRS315P$_{SSA2}$-SSA4** | LEU2 | (SHARMA AND MASISON 2008) |
| **pRS315P$_{SSA2}$-SSA42** | LEU2 | This study |
| **pRS315P$_{SSA2}$-SSA24** | LEU2 | This study |
| **pRS416P$_{GPD}$-His$_6$SSA2** | URA3 | (GUPTA *et al.* 2018) |
| **pRS416P$_{GPD}$-His$_6$SSA4** | URA3 | (GUPTA *et al.* 2018) |
| **pPROEXHTV-YDJ1** | Ampicillin | (SHARMA AND MASISON 2011) |
| **pET29bHTV-HSP82** | Kanamycin | This study |
| **pET29bHTV-STI1** | Kanamycin | This study |

731

732

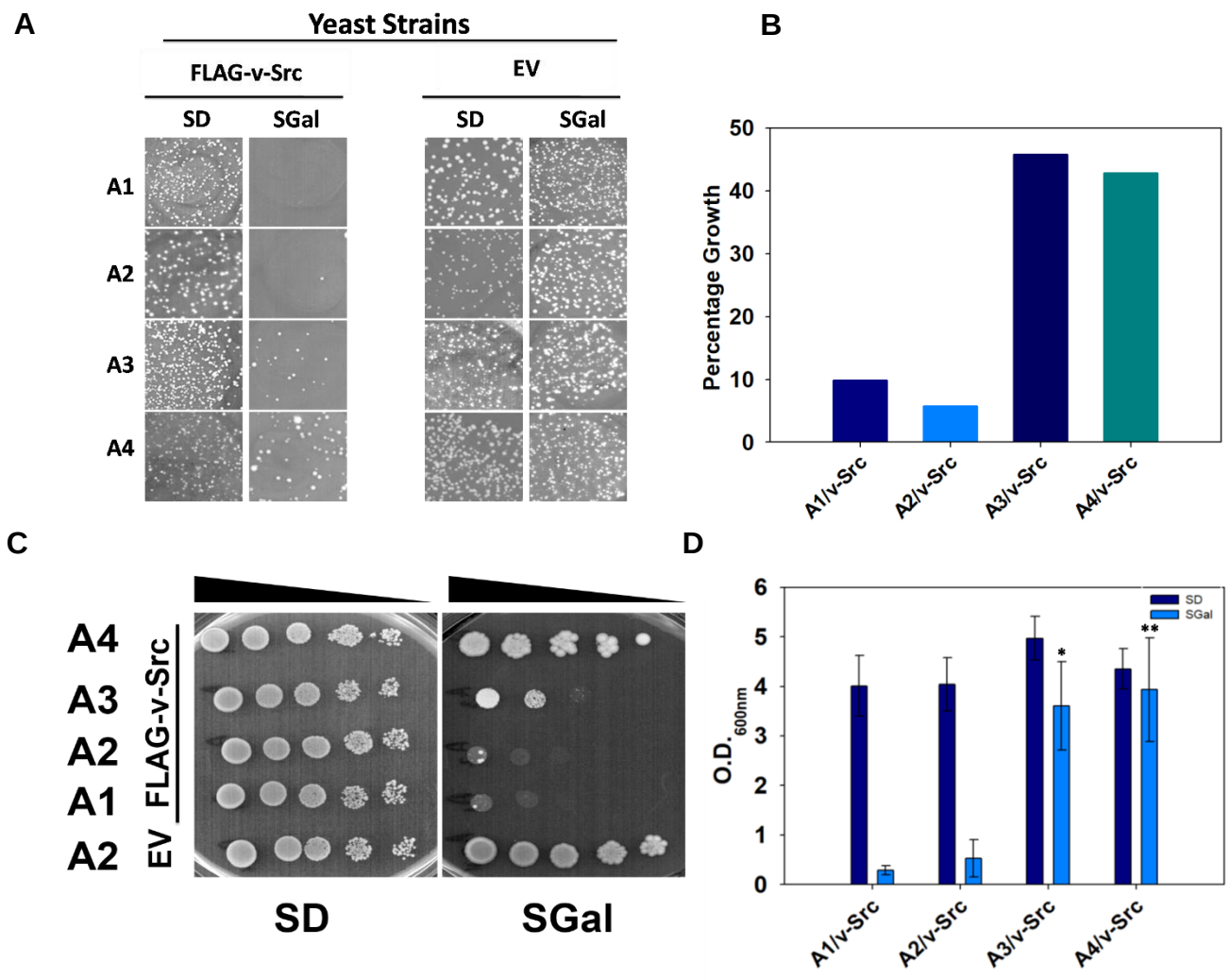


**Figure 1: Strains expressing Ssa3 or Ssa4 showed reduction in v-Src toxicity. (A)** *S.cerevisiae* strains A1-A4 were transformed with pRS316 (EV) or pRS316$P_{GAL1}$-FLAG-v-Src (FLAG-v-Src). Shown is growth of transformants onto SD and SGal solid media after 3 and 5 days respectively at 30°C. **(B)** Graph represents percentage number of colonies grown onto SGal growth media. Equal number of cells were plated onto SD and SGal media and percentage growth onto SGal was calculated with respect to SD media **(C)** Cells grown in selective liquid SD media were washed and serially diluted onto SD and SGal media. Shown is growth after 4 days of incubation at 30°C. **(D)** 5-6 transformants were pooled and grown in selective liquid SD media. Cells were re-inoculated at 0.02 $O.D._{600nm}$ into SD or SGal media. Shown is the $O.D._{600nm}$ of cell culture after 72 hours of incubation at 30°C. Error bar represents standard deviation from 3 different biological replicates. P-values were calculated using *t*-test and A2 as a control.

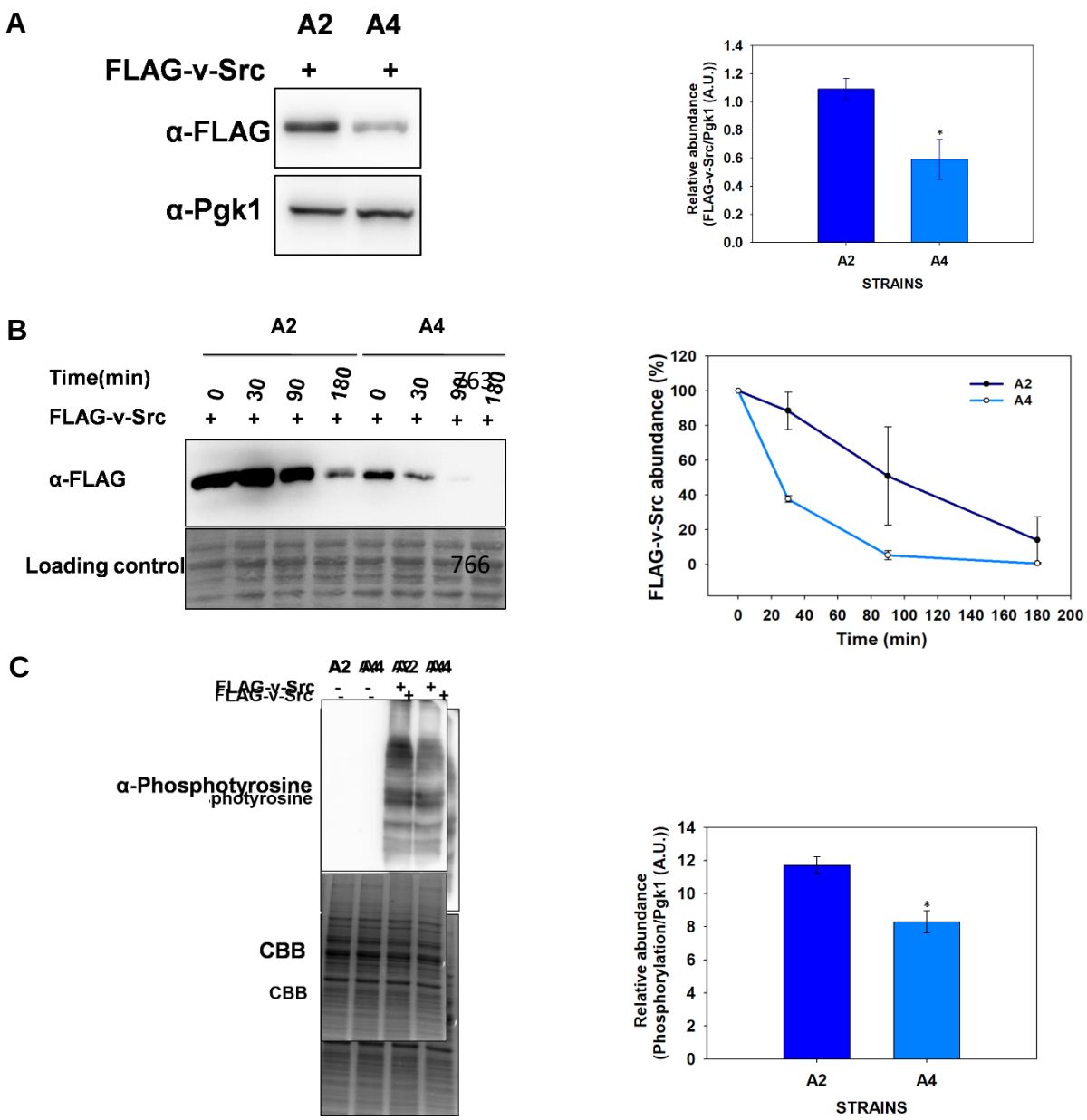


**Figure 2: The v-Src activity and its degradation in A4 and A2 strains. (A)** The v-Src expression was induced for 12hours, and its abundance was monitored in cellular lysate with anti-FLAG antibody. **(B)** The v-Src expression was induced for 12 h in SGal media. Cells were then shifted to non-inducible SD liquid media and v-Src abundance was chased at indicated time interval with anti-FLAG antibody. **(C)** The equal amount of cellular lysate from A2 or A4 strains expressing v-Src was probed with anti-phosphotyrosine antibody. Panel towards right depicts quantification of respective immunoblots. Error bar represents standard deviation from 3 different biological replicates. P-values were calculated using *t*-test and A2 as a control.

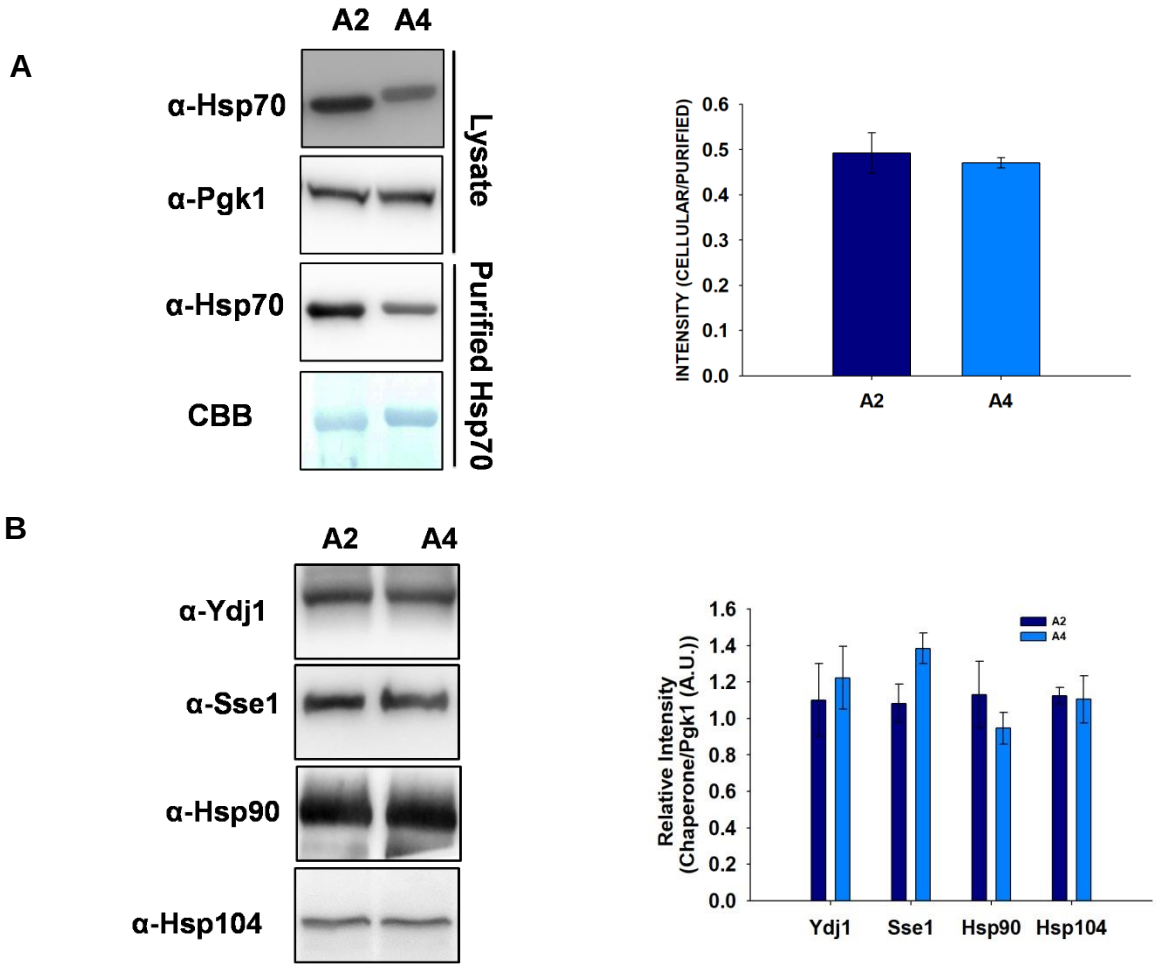


**Figure 3: A2 and A4 strains show similar abundance of major chaperones**: Yeast lysate was prepared from indicated strains overexpressing v-Src for 12 h. **(A)** Equal amounts of the cellular lysate (upper panel) or purified $His_6$-tagged Ssa Hsp70 (Lower panel) was loaded onto 10% SDS-PAGE and probed with anti-Hsp70 antibody. Coomassie Brilliant Blue (CBB) was used to stain purified Hsp70s as loading control. **(B)** Equal amount of cellular lysate from indicated strains was probed with antibodies against Ydj1, Sse1, Hsp90 or Hsp104. Right panel shows quantification of respective immunoblots. Error bar represents standard deviation from 3 different biological replicates.

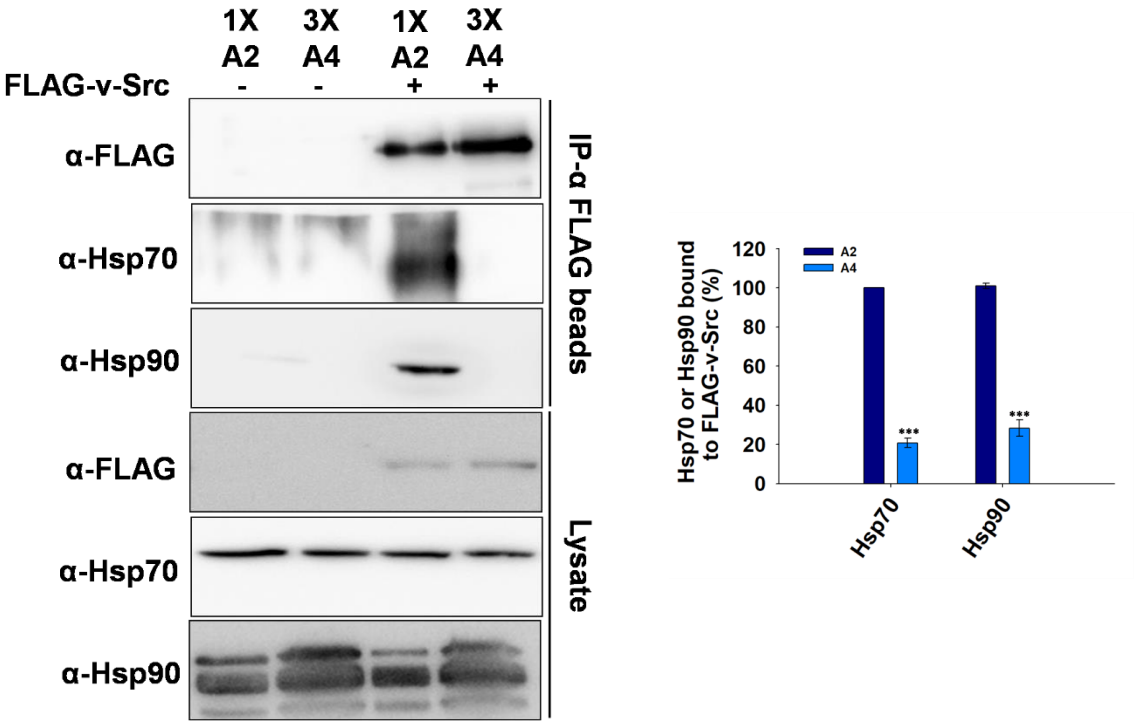


**Figure 4: The v-Src interaction with Hsp70 and Hsp90 using immunoprecipitation studies.** The indicated strains were grown in selective SGal media for v-Src expression. The cells were lysed, and lysate was incubated with anti-FLAG antibody immobilized beads. The immunoprecipitated proteins were probed with indicated antibodies. Right panel shows quantification of respective immunoblots. Error bar represents standard deviation from 3 different biological replicates. P-values were calculated using *t*-test and A2 as a control.

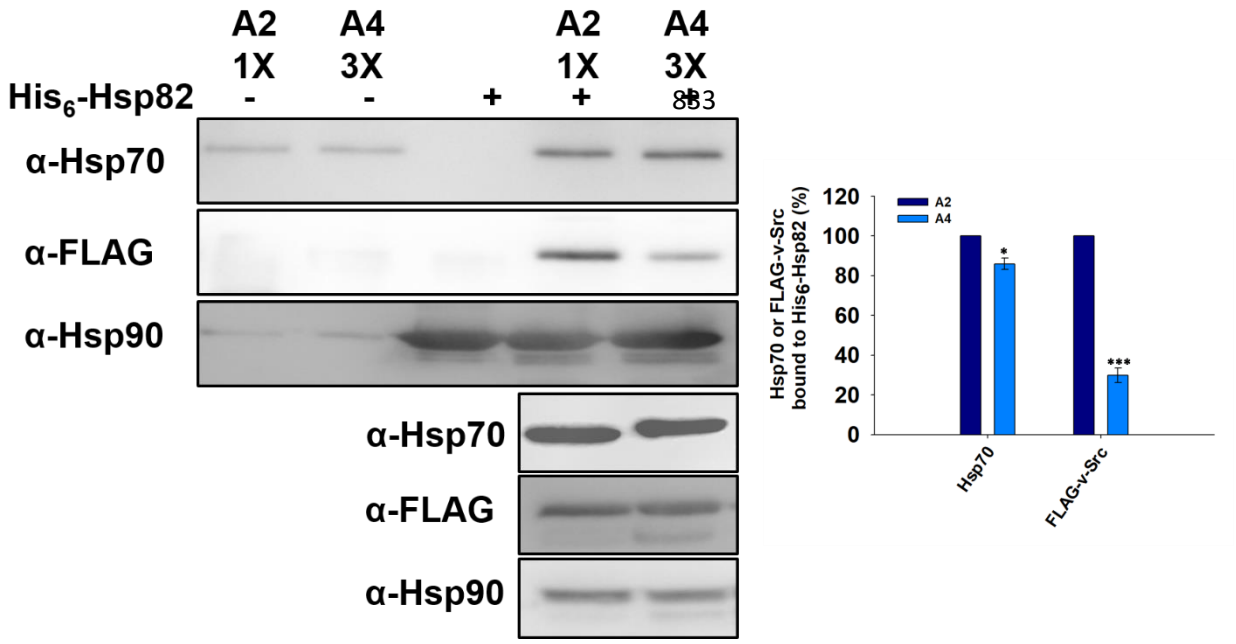


**Figure 5: The Hsp82 interaction is similar with Ssa2 and Ssa4 isoforms of Hsp70.** The purified $His_6$-Hsp82 was adsorbed onto Cobalt metal affinity resin and further incubated with yeast lysate from A2 or A4 strains expressing FLAG-v-Src. The bound fractions were probed for Ssa Hsp70s, v-Src or Hsp82 with anti-Hsp70 antibody, anti-Hsp90 antibody or anti-FLAG antibody respectively. Panel towards right depicts quantification of respective western blots. Error bar represents standard deviation from 3 different biological replicates. P-values were calculated using *t*-test and A2 as a control.

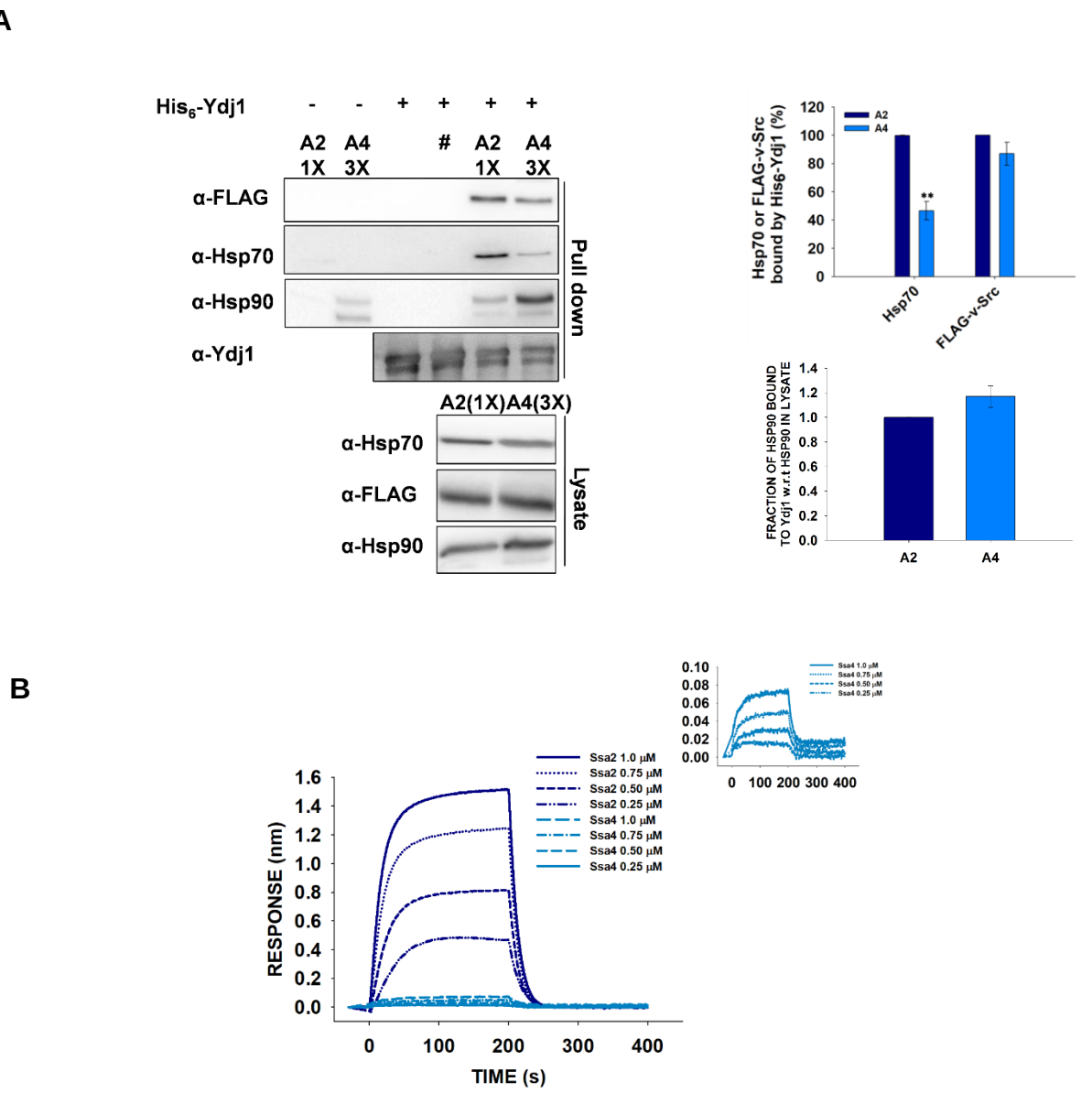


**Figure 6: The Ydj1 interaction is stronger with Ssa2 than Ssa4. (A)** The $His_6$-Ydj1 immobilized beads were incubated with yeast lysate from A2 (1X) or A4 (3X) cells expressing FLAG tagged v-Src. The bound proteins were probed with anti-FLAG, anti-Hsp70, anti-Hsp90 or anti-Ydj1 antibody. Relatively higher amount of Hsp70 from A2 strain was detected indicating a stronger interaction of Ydj1 with Ssa2 than Ssa4. Panel towards right depicts quantification of respective western blot. $^{\#}$A mutant of Ydj1 ($His_6$-Ydj1(H34Q)) was used as negative control. **(B)** The BLI sensogram showing interaction of Ydj1 with increasing concentrations of Hsp70 isoforms (Ssa2 or Ssa4) as analyte. A much stronger interaction of Ydj1 with Ssa2 than Ssa4 was observed at similar concentrations of the two Hsp70 isoforms. Inset shows the zoomed-in view of Ydj1 interaction with Ssa4. The labels are represented in same order as magnitude of curve. Error bar represents standard deviation from 3 different biological replicates. P-values were calculated using *t*-test and A2 as a control.

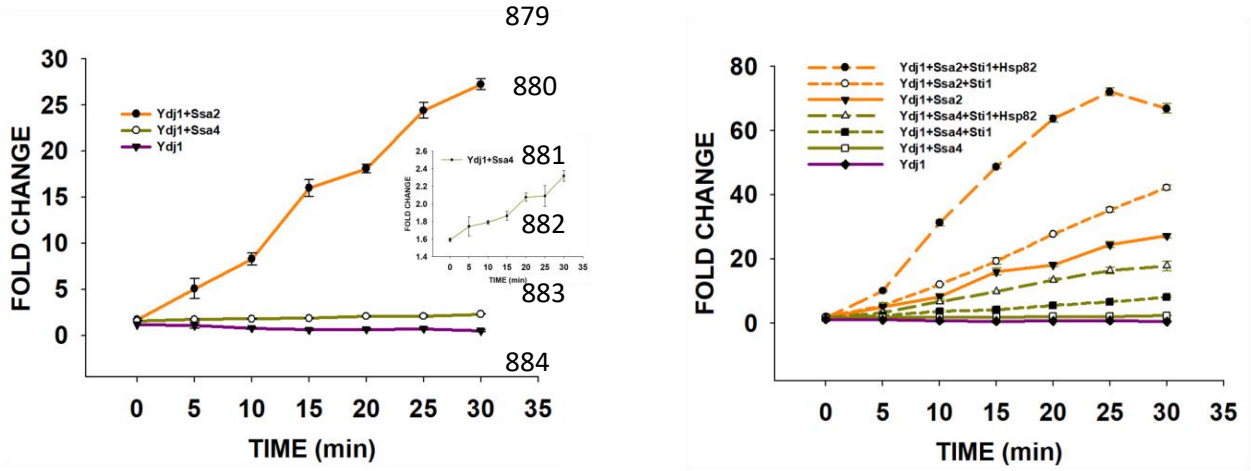


**Figure 7: Ssa2 has higher luciferase refolding activity compared to Ssa4: (A)** Luciferase was denatured at 45°C, and refolded in the presence of Ssa2 or Ssa4 and Ydj1.As shown fraction of luciferase that refolded is higher in the presence of A2 than A4. **(B)** The denatured luciferase (40nM) was incubated in the presence of 0.3µM Ydj1, 0.5µM Hsp70 (Ssa2 or Ssa4), 2.4µM Sti1 and 0.9µM Hsp82, and the refolding was monitored by measuring increase in luminescence. The luciferase refolding curves for Ydj1:Ssa2, Ydj1:Ssa4 and Ydj1 alone in Panel B are adapted from Panel A for comparison. The labels are represented in same order as magnitude of curve. Error bar represents standard deviation from 3 different biological replicates.

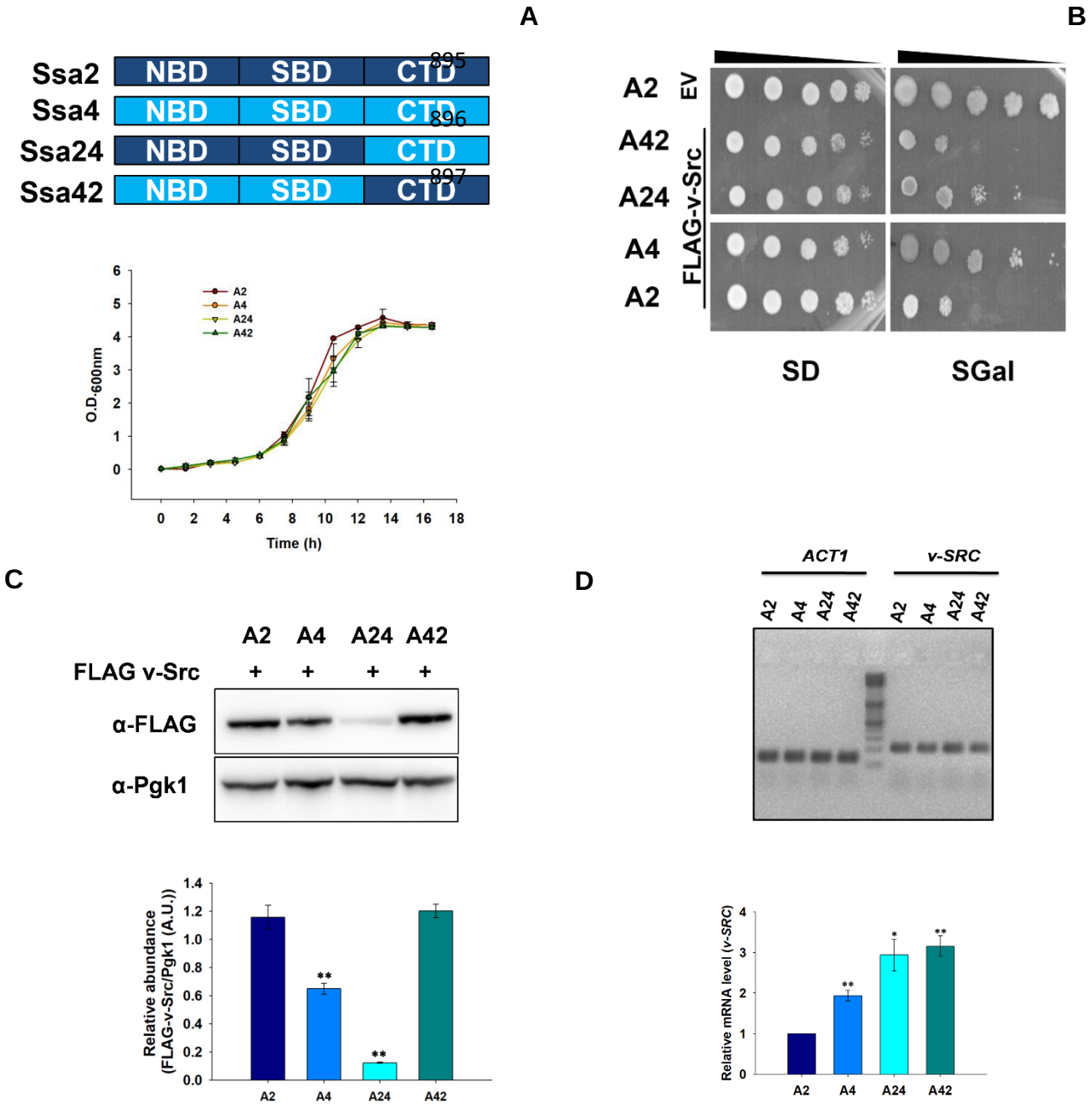


**Figure 8: C-terminal domain of Hsp70 governs its specificity for v-Src maturation: (A)** Upper Panel shows schematics of designed hybrid Hsp70 proteins. Amino acid sequence at hybrid junction in Ssa24 and Ssa42 are 537-538 of Ssa2 and 538-539 of Ssa4 respectively. Lower Panel shows growth curve of indicated strains in liquid YPAD media. **(B)** Shown is the growth of indicated strains onto solid SD or SGal media after 5 days of incubation at 30°C. **(C)** Immunoblot showing steady state expression of FLAG tagged v-Src or Pgk1 (as control) in indicated strains. **(D)** The relative abundance of mRNA encoding v-Src in indicated strains as measured using qRT-PCR. The qRT-PCR was carried out using primers specific for *v-SRC* or *ACT1* (as control). Lower panel in (C) and (D) shows relative quantification. Error bar represents

standard deviation from 3 different biological replicates. P-values were calculated using *t*-test and A2 as a control.

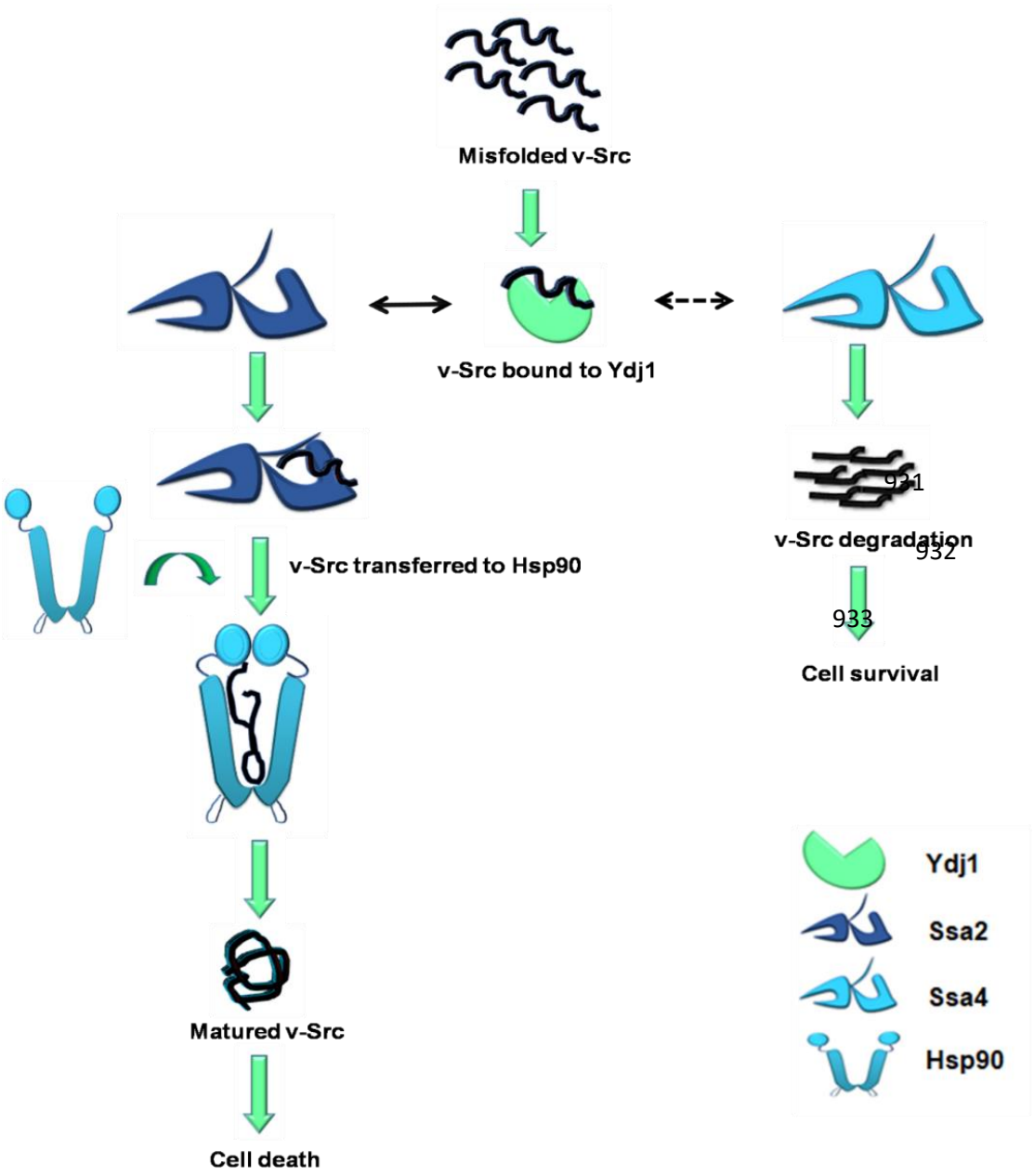


**Figure 9: Model of how Ydj1 regulates activity of Ssa2 and Ssa4.** Misfolded v-Src interacts with Ydj1. Ydj1 further recruit v-Src to Hsp70. Solid black arrow represents transfer of v-Src to Ssa2 while dashed arrow represents that Ydj1 is not able to transfer v-Src to Ssa4. Lack of Ydj1-Ssa4 interaction results in degradation of v-Src and cell survival in Ssa4 background. Hsp90 interacts with Ssa2, thus v-Src is transferred to Hsp90 and gets matured. v-Src maturation through Hsp90 results in cell death in Ssa2 background.

## Supplementary figures

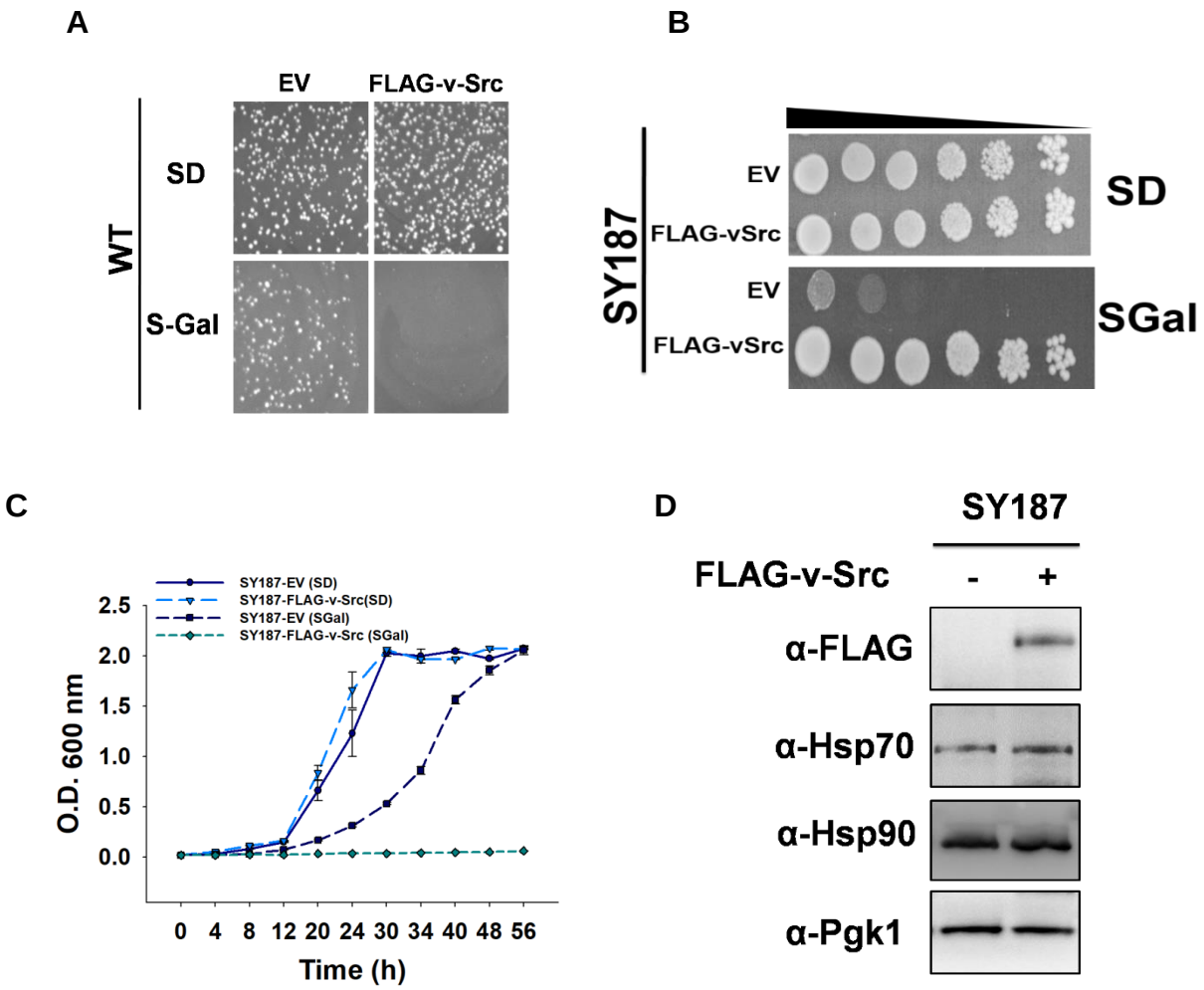


**Figure S1**: **v-Src overexpression is toxic to wt *S.cerevisiae* strain SY187. (A)** *S.cerevisiae* strain SY187 was transformed with pRS316 (EV) or pRS316$P_{GAL}$-FLAG-v-Src (FLAG-v-Src). Shown is growth of transformants onto solid SD and SGal media after 3-5 days of incubation at 30°C. **(B)** Above strains were grown overnight into selective liquid SD media. Cells were serially diluted and spotted onto solid SD or SGal media. Shown is the growth after 5 days of incubation at 30°C. **(C)** Growth assay to monitor growth of indicated strains in liquid media. **(D)**

976 The immunoblot showing expression level of v-Src, Hsp70 and Hsp90 in cellular lysate of
977 indicated strains. Error bar represents standard deviation from 3 different biological replicates.

978

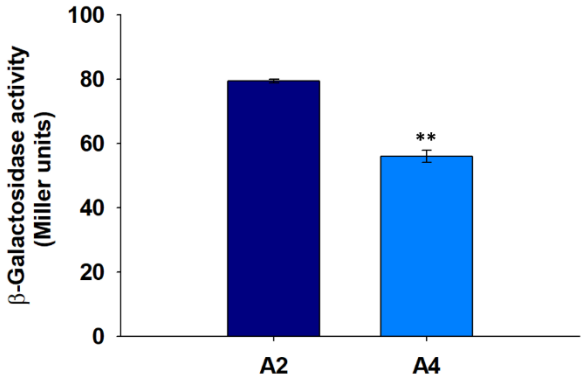


**Figure S2: Ste11 kinase maturation is impaired in A4 strain:** Indicated strains were transformed with plasmid encoding PRE-lacZ. Transformants were pooled and grown into liquid SD media until $O.D._{600nm}$ of 1.0. Cells were then treated with α-factor for 6 hours before monitoring lacZ activity. Error bar represents standard deviation from 3 biological replicates. P-values were calculated using *t*-test and A2 as a control.

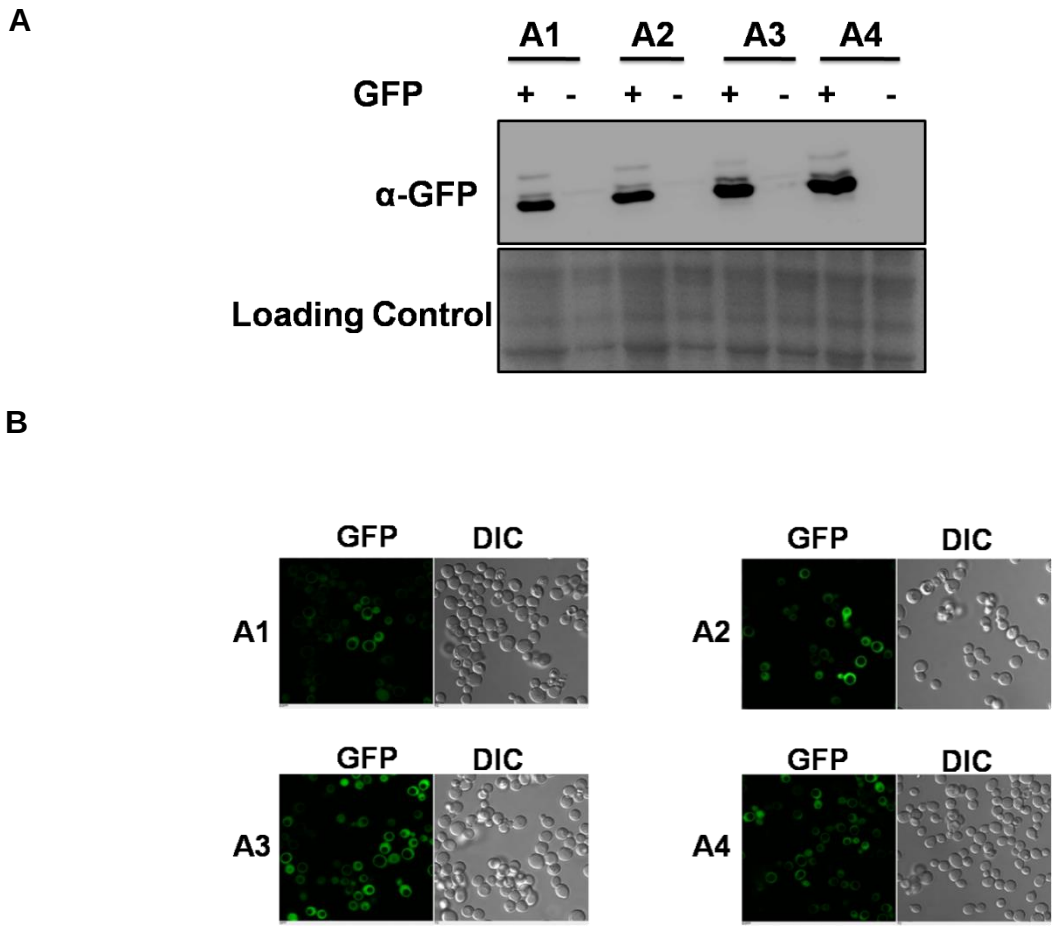


**Figure S3: *S.cerevisiae* strains A1-A4 show similar levels of GFP from GAL1 promoter.** The strains A1, A2, A3 and A4 were transformed with pRS316$P_{GAL1}$-GFP. About 5-6 transformants were pooled into SD media and further grown into SGal media for 6h. **(A)** Cellular lysate was probed with anti-GFP antibody. **(B)** The cells were examined using fluorescence microscopy.

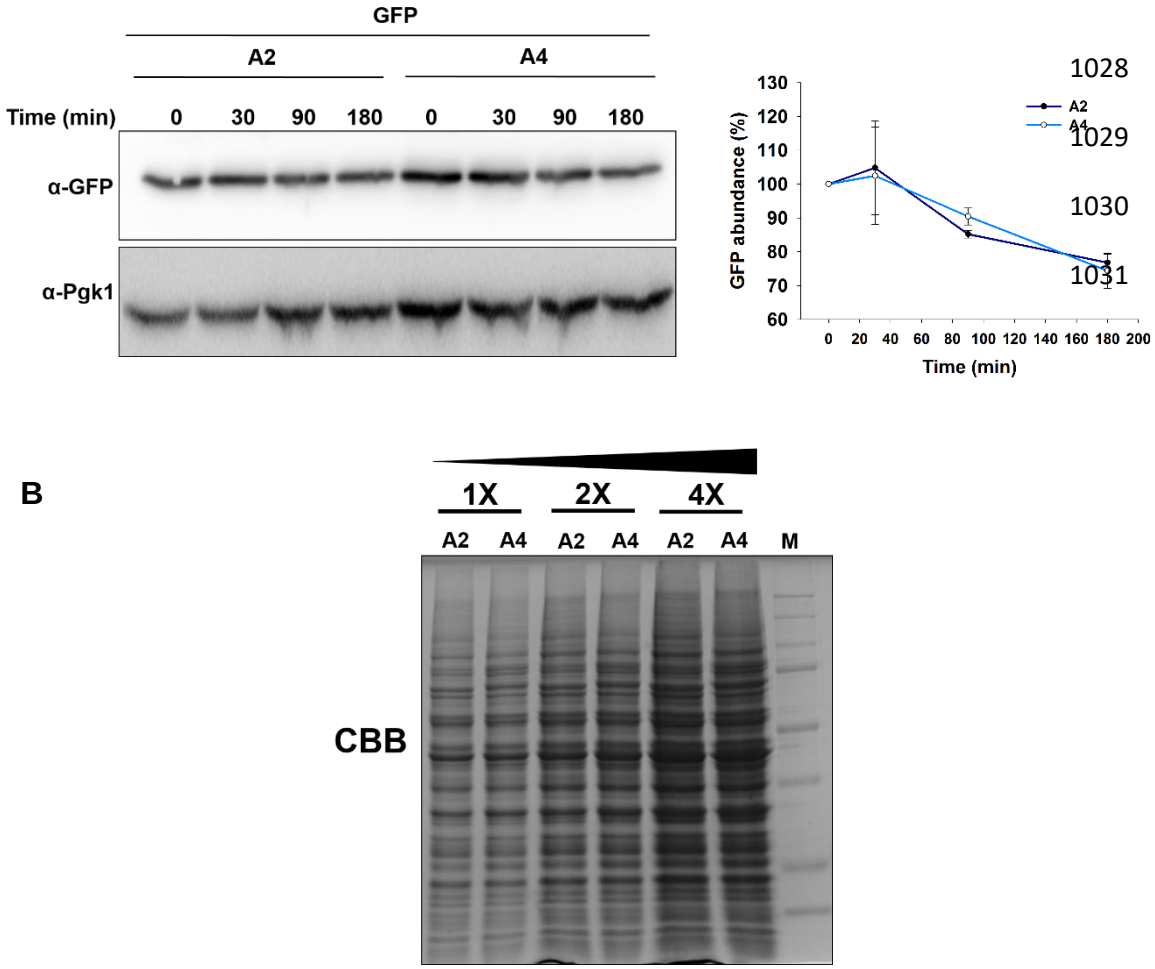


**Figure S4: Protein homeostasis in A2 and A4 strains. (A)** The GFP was expressed from galactose inducible promoter. The expression was induced for 12 h in SGal media. Cells were then shifted to non-inducible SD liquid media. Cells were collected at indicated time intervals, and cellular lysate was probed with anti GFP antibodies. Right panel shows quantification of respective immunoblot. Error bar represents standard deviation from 3 different biological replicates. **(B)** Equal $O.D._{600nm}$ (1.0) cells were collected, and lysate was fractionated onto SDS-PAGE. Shown is the coomassie stained SDS-PAGE.

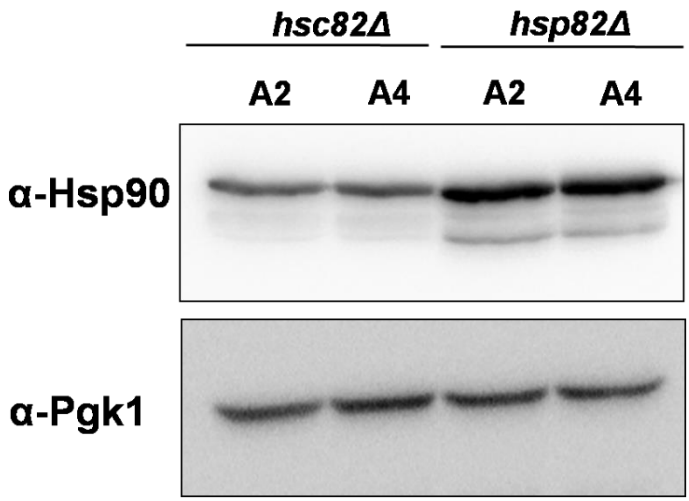


**Figure S5: Anti Hsp90 antibody detects both Hsc82 and Hsp82:** Lysate was prepared from *hsc82Δ* and *hsp82Δ* in A2 and A4 background. Lysate was fractionated onto 12% SDS-PAGE and further analyzed by anti-Hsp90 antibody.

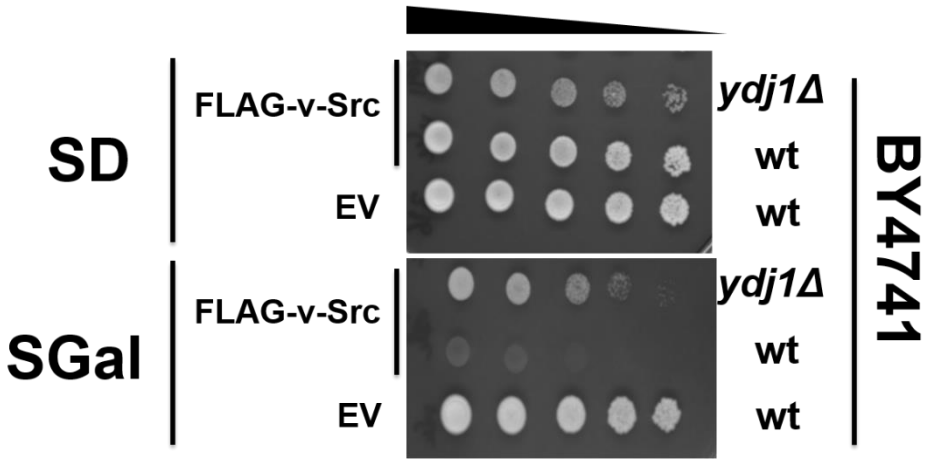


**Figure S6: The YDJ1 deletion suppresses v-Src mediated toxicity.** Indicated strains were transformed with pRS316$P_{GAL1}$-FLAG-vSrc and were further spotted onto solid SD and SGal media. Shown is growth after 5 days of incubation at 30°C.

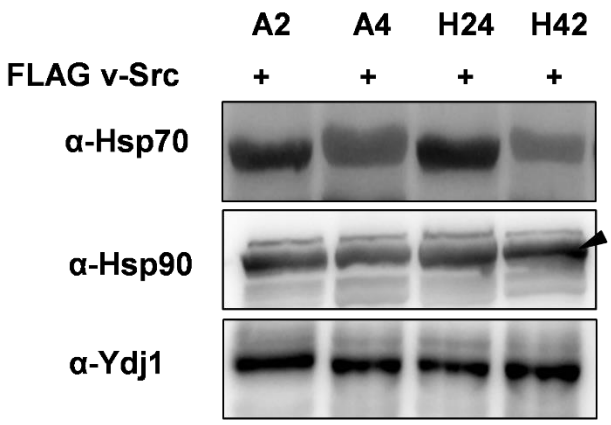


**Figure S7: Hybrid Ssa Hsp70s, Hsp90 and Ydj1 are expressed at similar level.** Yeast lysate was prepared from indicated strains overexpressing v-Src for 12hours Whole cell lysate from indicated strains was probed with antibodies against Hsp70, Hsp90 and Ydj1. Arrowhead represents Hsp90 band.

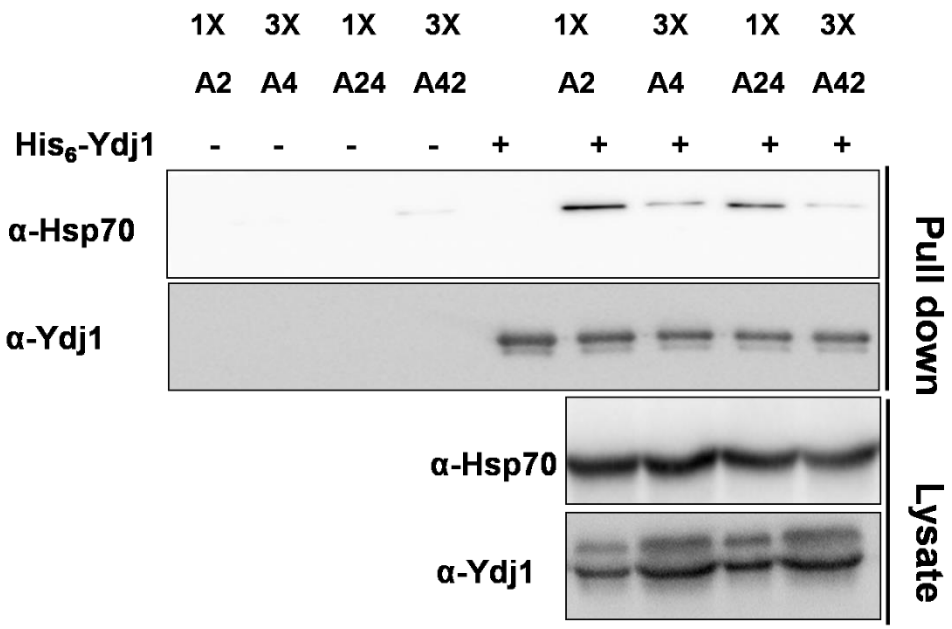


**Figure S8: Hybrids A24 and A42 both show no interaction with Ydj1.** $His_6$-Ydj1 was bound onto Co-NTA beads and further incubated with lysate from A2, A4(3X), A24 and A42(3X). Bound fractions were eluted with EDTA and further probed with anti-Ydj1 and anti-Hsp70 antibody.

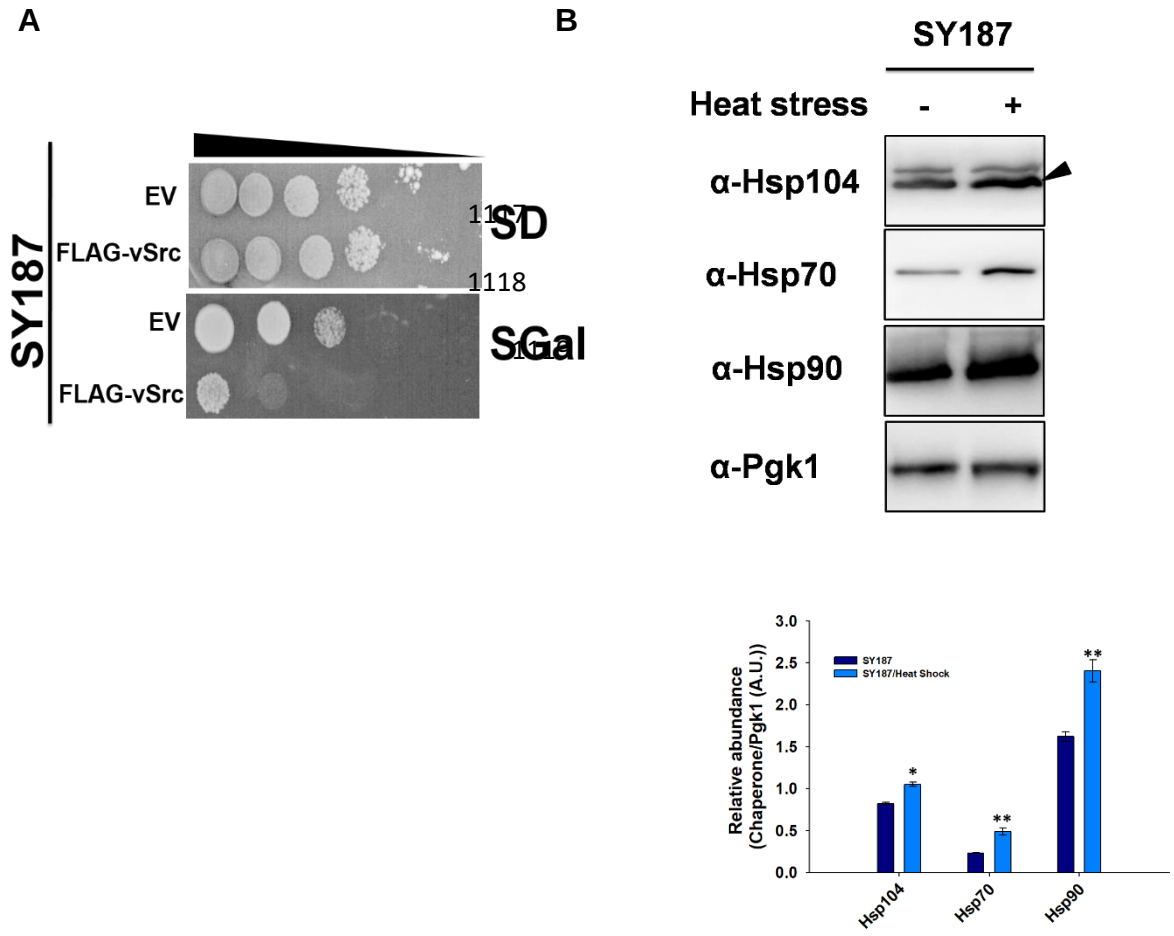


**Figure S9**: **Heat stress has no effect on v-Src mediated toxicity in wt strain. (A)** Indicated strains were grown into selective SD media. Cells were washed and serially diluted onto solid SD and SGal media. Plates were further incubated at 37°C. Shown here is growth after 6 days of incubation at 37°C. **(B)** Immunoblot showing increase in the level of Hsp104, Hsp70 and Hsp90 upon heat stress. For heat stress, wtSY187 strain was grown into liquid SD media at 30°C followed by incubation at 37°C for 2hours before preparing yeast lysate for immunoblot analysis. Arrowhead represents Hsp104 band. Error bar represents standard deviation from 3 different biological replicates. P-values were calculated using *t*-test and A2 as a control.